1 ***Discoidin domain receptor* regulates ensheathment, survival, and caliber of peripheral**
2 **axons**

3 Megan M. Corty[1], Alexandria P. Lassetter[1], Jo Q. Hill[2], Amy E. Sheehan[1], F. Javier Bernardo-
4 Garcia[2], Graeme W. Davis[2], Sue A. Aicher[3], Marc R. Freeman[1]

5 [1]Vollum Institute, Oregon Health & Science University, Portland, OR, 97239, USA

6 [2] Department of Biochemistry and Biophysics, Kavli Institute for Fundamental Neuroscience,
7 University of California, San Francisco, San Francisco, CA 94158, USA

8 [3]Department of Chemical Physiology & Biochemistry, Oregon Health & Science University,
9 97239, Portland, OR, USA

10 Correspondence: freemmar@ohsu.edu

11 Key Words: wrapping glia, *Drosophila*, Remak Schwann cell, Multiplexin, axon ensheathment

12

13

1

14 **Abstract**

15   Invertebrate axons and small caliber axons in mammalian peripheral nerves are

16 unmyelinated but still ensheathed by glia. How this type of ensheathment is controlled and its

17 roles in supporting neuronal function remain unclear. We performed an *in vivo* RNAi screen in

18 *Drosophila* to identify glial genes required for axon ensheathment and identified the conserved

19 receptor tyrosine kinase Discoidin domain receptor (Ddr). In larval peripheral nerves, loss of

20 Ddr resulted in incomplete ensheathment of axons. We found a strong dominant genetic

21 interaction between *Ddr* and the fly type XV/XVIII collagen *Multiplexin (Mp)*, suggesting Ddr

22 functions a collagen receptor to drive wrapping of axons during development. Surprisingly,

23 while ablation of glia that wrap axons severely impaired larval motor behavior, incomplete

24 wrapping in *Ddr* mutants was sufficient to support basic circuit function. In adult nerves, loss of

25 Ddr from glia decreased long-term survival of sensory neurons and significantly reduced axon

26 caliber without overtly affecting ensheathment. Our data establish a crucial role for non-

27 myelinating glia in peripheral nerve development and function across the lifespan, and identify

28 Ddr as a key regulator of axon-glia interactions during ensheathment.

29

30 **Introduction**

31   In complex nervous systems, specialized glial cells ensheathe long axons, and this

32 wrapping can take many forms. Myelination is the most studied type of ensheathment, but

33 unmyelinated axons make up the majority (~70%) of axons in human peripheral nerves (Ochoa

34 and Mair, 1969; Schmalbruch, 1986). Vertebrate Remak Schwann cells ensheathe and separate

35 unmyelinated axons from one another. These small caliber axons include many types of sensory

36 neuron axons, including nociceptive c-fibers and autonomic axons (Griffin and Thompson,

37 2008). Remak Schwann cells are positioned to mediate fundamental aspects of nerve

38 development and sensory biology, and be important modulators of neurological conditions

39 affecting the peripheral nervous system (PNS) including peripheral neuropathies and nerve

40 injuries. However, Remak Schwann cells have remained understudied, in part due to a lack of

41 selective genetic tools to specifically target this population.

42   In *Drosophila,* axons in peripheral nerves are ensheathed by specialized wrapping glia in

43 a manner analogous to vertebrate Remak bundles (Figure 1A-B). *Drosophila* larval abdominal

44 nerves project out of the ventral nerve cord in each segment and contain both motor and sensory

45 neuron axons surrounded by multiple glial layers: the outermost perineurial glia, then

46 subperineural glia, and finally axon-associated wrapping glia (Hilchen et al., 2013; Matzat et al.,

47 2015; Stork et al., 2008)(Figure 1A,B). Wrapping is progressive throughout larval life. In

48 embryos, axons are initially tightly fasciculated without intervening glial processes. Wrapping

49 progresses such that by third instar axons are wrapped either individually or in small bundles by

50 wrapping glia membrane (Figure 1B, C) (Matzat et al., 2015). This process mirrors vertebrate

51 nerve development when Schwann cells perform radial sorting of axons that are initially tightly

52 fasciculated (Monk et al., 2015) and a growing body of evidence that demonstrates a high degree

53 of cellular and molecular conservation between ensheathment mechanisms in *Drosophila* and

54 vertebrates (Ghosh et al., 2013; Matzat et al., 2015; Mukherjee et al., 2020; Petley-Ragan et al.,

55 2016; Xie and Auld, 2011). This Remak-like type of multi-axonal ensheathment is thought to

56 represent an ancient form of axon-glial association, and the emerging cellular and molecular

57 conservation of multiple aspects of peripheral nerve biology make *Drosophila* wrapping glia a

58 promising model to study non-myelinating ensheathment *in vivo*.

59   Beyond simply insulating individual axons, glia that ensheathe axons also regulate

60   neuronal development, maintenance, and function throughout an animal's lifespan. Myelination

61   can alter the distribution of axonal proteins, increase axon caliber, and is important for trophic

62   and metabolic support of long axons, though the precise mechanisms by which myelinating glia

63   perform all of these functions remain incompletely understood (Nave, 2010). Recent work

64   supports the notion that Remak Schwann cells play similar important roles: perturbation of

65   Schwann cell metabolism results in axon degeneration, with small caliber, Remak-ensheathed

66   axons degenerating earlier than myelinated ones (Beirowski et al., 2014). Although Remak

67   Schwann cells were not targeted selectively, these observations support the notion that

68   unmyelinated axons are also reliant on glial support.

69   Here we take advantage of *Drosophila* wrapping glia as a model to identify new

70   molecular regulators of glial ensheathment and support of axons. Through an RNAi-based

71   screen, we identify *Discoidin domain receptor* (*Ddr*) as crucial for glial ensheathment in larval

72   nerves. We demonstrate that wrapping glia are essential for normal nerve function and behavior

73   by developing a new Split-Gal4 intersectional driver to genetically ablate larval wrapping glia,

74   which results in severely impaired crawling behavior. Surprisingly, while loss of Ddr results in

75   incomplete wrapping, it did not result in overt effects on behavior, arguing that even partial

76   ensheathment is sufficient to support normal nerve function. In adult nerves, loss of *Ddr* results

77   in reduced long-term survival of peripheral sensory neurons and reduced axon caliber without

78   affecting ensheathment. Ddr is therefore a new glial regulator of axon caliber *in vivo*. Finally,

79   we identify the collagen multiplexin (Mp) as a potential ligand for Ddr in driving wrapping

80   during development, suggesting that Ddr-collagen interactions are critical regulators of axon

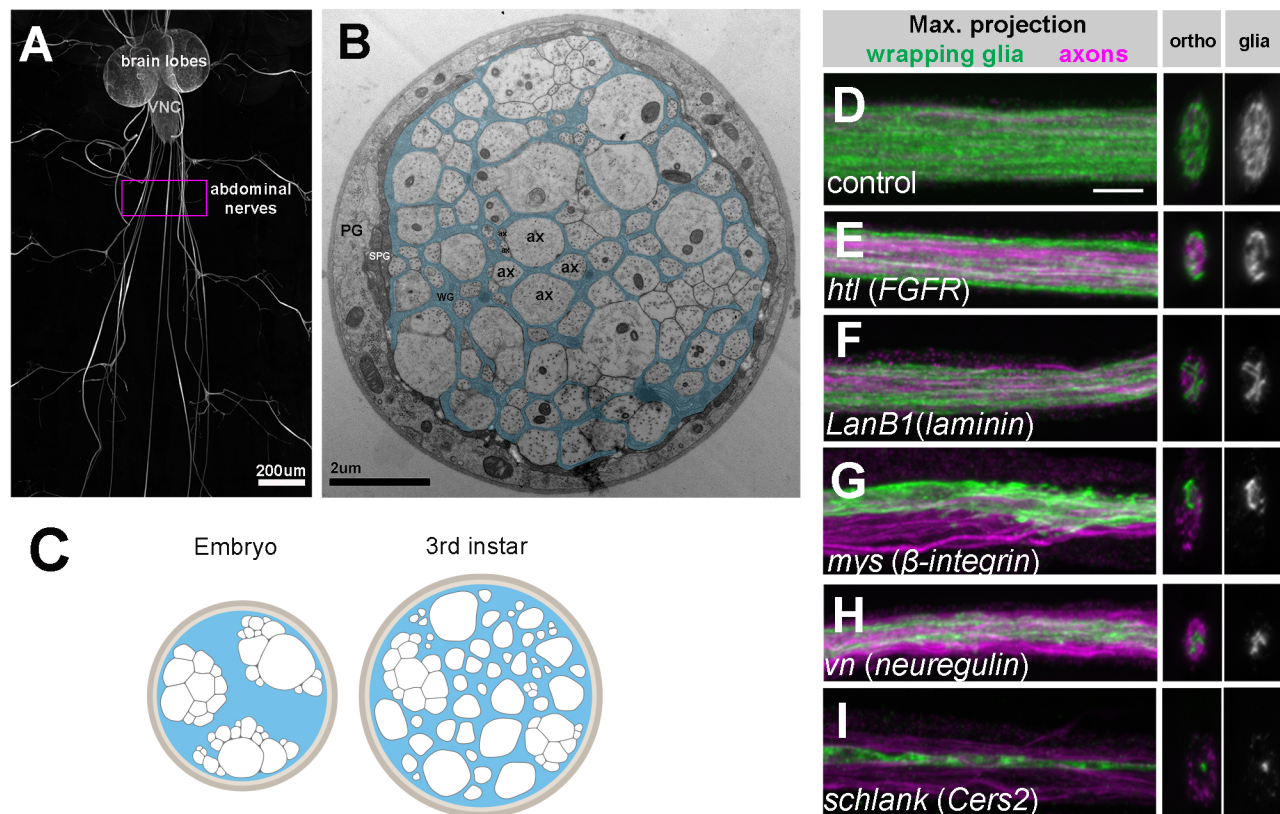81   ensheathment and glial support of neurons.

FIGURE 1

Figure 1: *Drosophila* wrapping glia are a model of multi-axonal ensheathment

(A) Confocal image showing a 3rd instar larval nervous system including the brain, ventral nerve cord (VNC), and peripheral nerves as labeled in a *nrv2-Gal4>UASmCD8:GFP* animal. This driver labels wrapping glia in the nerves as well as some subtypes of CNS glia in the brain and VNC. Boxed region corresponds to the approximate area imaged for glial morphology analysis. **(B)** TEM cross-section of a third instar larval nerve. Light, round profiles of larval axons (ax) are surrounded by darker (pseudo-colored cyan) wrapping glia. Subperineurial (SPG) and perineurial glia (PG; not colored) form the outer layers of the nerve, which is coated by a neural lamella of ECM proteins. **(C)** Schematic representation of larval nerve cross sections at hatching and 3rd instar stages illustrating that wrapping is progressive over larval development. **(D-H)** RNAi against genes with known roles in wrapping glia and vertebrate glia development results in visible morphological defects at the light level. Wrapping glia are labeled with myr:tdTomato driven by *nrv2-Gal4* (pseudo-colored green). A subset of sensory axons are labeled with anti-Futsch (magenta). A maximum confocal projection of the nerve is shown in the left panel. The ortho panel shows the nerve cross section, and the glia channel is the isolated wrapping glial channel in cross section. Scale bar 5μm. **(D)** Control nerves show fairly uniform, honeycomb-like glia membrane coverage of the nerve cross section. **(E)** Wrapping glial knockdown of *heartless*, an FGF Receptor homolog, shows incomplete glial coverage of the nerve cross section. **(F)** Knockdown of *lanB1*, a laminin homolog, causes impaired cross section coverage. **(G)** Knockdown of the β-integrin homolog *myospheroid* causes highly abnormal glia morphology where glia fail to cover the entire nerve. **(H)** Knockdown of the neuregulin homolog, *vein*, results in impaired glia coverage of the nerve cross section. **(I)** Knockdown of *schlank*, a Ceramide Synthetase-2 homolog, results in thin stringy glia that does not appear to wrap axons at all.

5

82

83   RESULTS

84   **Morphology based RNAi screen identifies *Ddr* as a regulator of wrapping glia development**

85   To identify genes that are required in glia for normal ensheathment of axons, we

86   conducted a morphology based RNAi screen to systematically knock down genes in wrapping

87   glia and look for changes in glial morphology in third instar larval nerves (Matzat et al. 2015;

88   Stork et al. 2008). To visualize and manipulate wrapping glia, we used the well-established

89   *nrv2-Gal4* driver line which, within the PNS, is strongly and exclusively expressed in wrapping

90   glia (Stork et al., 2008; Xie and Auld, 2011). We expressed a membrane bound marker (*UAS-*

91   *myr:tdTomato*) to visualize wrapping glia morphology and *UAS-RNAi* constructs from the

92   Vienna *Drosophila* Resource Collection to knock down genes selectively in wrapping glia

93   throughout development. In total, we screened a collection of ~2000 RNAi lines, which comprise

94   the majority of transmembrane, secreted, and signaling proteins in the fly genome and included

95   the fly homologs of ~200 genes strongly expressed in the developing mouse oligodendrocyte

96   lineage based on available RNA-seq data (Zhang et al., 2014).

97   Using spinning disk confocal microscopy and examination of nerve cross sections, we

98   found that wild type wrapping glia morphology in third instar larvae includes membrane

99   coverage throughout the interior of the nerve with small, regularly spaced gaps like a tight

100   honeycomb (Figure 1D and Figure 2—figure supplement 1A,B). As a positive control for our

101   screen, we knocked down genes previously shown to be involved in wrapping glia development

102   including the neuregulin homolog *vein*, the FGF receptor *heartless*, integrin receptors, laminin,

103   and the ceramide synthetase gene, *schlank* (Franzdóttir et al., 2009; Ghosh et al., 2013;

104   Kottmeier et al., 2020; Matzat et al., 2015; Petley-Ragan et al., 2016; Xie and Auld, 2011), all of

6

105 which resulted in easily identifiable defects in axon ensheathment using confocal microscopy

106 (Figure 1E-I). Each of these genes have homologs that have been implicated in oligodendrocyte

107 and/or Schwann cell development, further arguing for strong molecular conservation among both

108 vertebrate and invertebrate axonal ensheathment mechanisms (Barros et al., 2009; Feltri et al.,

109 2002; Furusho et al., 2009; Lyons et al., 2005; Michailov et al., 2004; Pereira et al., 2009;

110 Stassart et al., 2013; Taveggia et al., 2005; Yu et al., 2009).

111   Among potential hits whose function had not previously been studied in either vertebrate

112 or invertebrate glia was the *Discoidin domain receptor* (*Ddr*) gene (Figure 2A). Knocking down

113 *Ddr* using two independent RNAi constructs led to altered wrapping glia morphology with the

114 nerve cross section incompletely covered by glial membrane, suggesting that axons were not

115 properly wrapped when *Ddr* was knocked down (Figure 2B-D). *Drosophila Ddr* encodes a

116 receptor tyrosine kinase homologous to vertebrate Ddr1 and Ddr2. In the mouse, Ddr1 is

117 expressed in Schwann cells and the oligodendrocyte lineage (Franco-Pons et al., 2006; Gerber et

118 al., 2021; Roig et al., 2010; Zhang et al., 2014), but direct roles for Ddr1in regulating

119 ensheathment of axons have not been reported. Thus, the results from our screen provide the

120 first functional indication that this receptor could be involved in regulating axonal wrapping.

121

Ddr mutants exhibit defects in axonal ensheathment

123   To confirm that *Ddr* is involved in wrapping glia development, we created mutant alleles

124 of *Ddr* using a CRISPR-Cas9 strategy. Briefly, using two gRNAs against widely spaced,

125 adjacent exons, we generated fly stocks in which an ~11kb region of the *Ddr* coding region was

126 excised near the 5' end (Figure 2A & 2H). We sequenced the resulting deletion lines to identify

127 mutants that resulted in frame shift mutations and early stop codons. *Ddr* encodes two potential
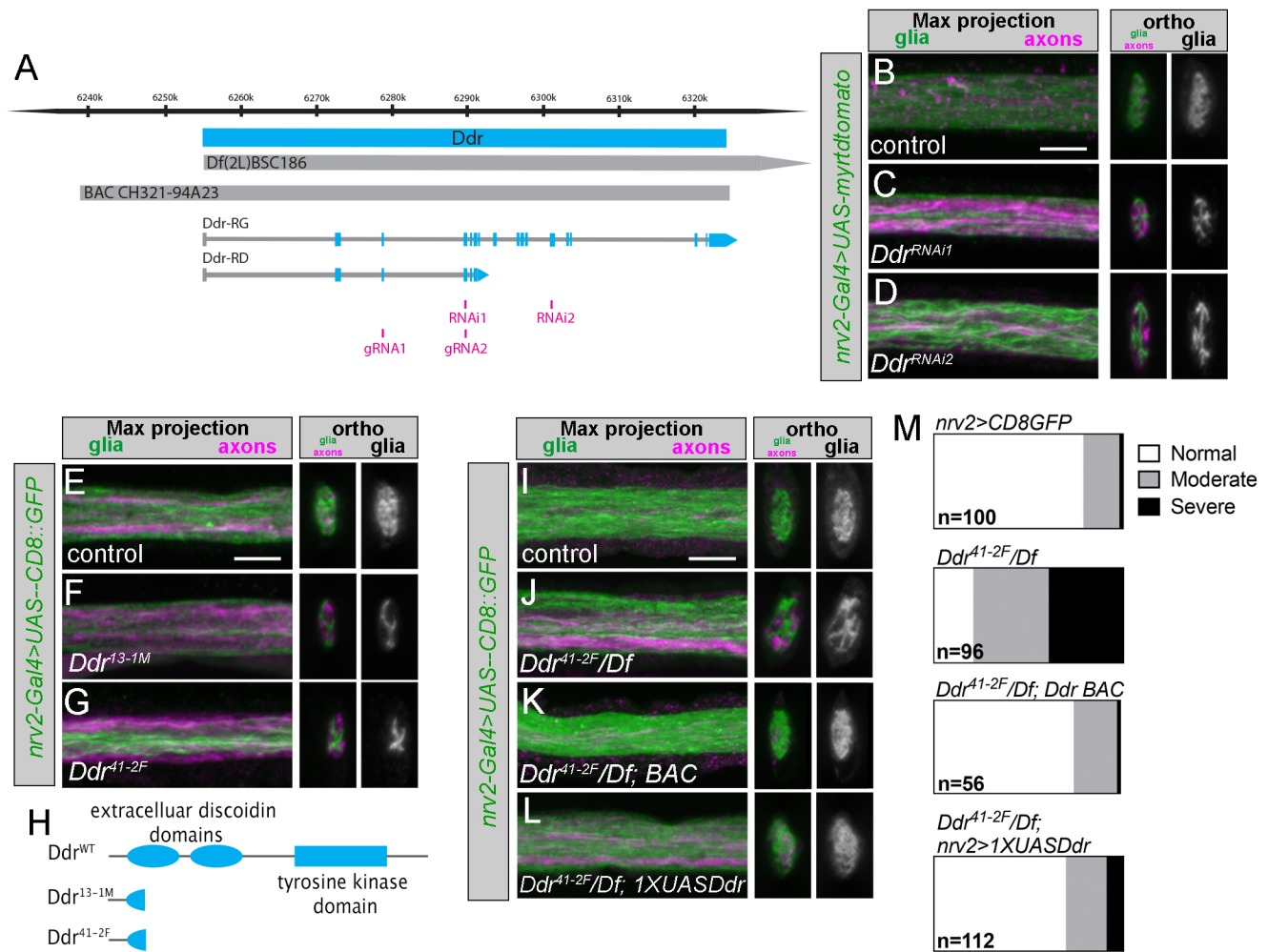
FIGURE 2

Figure 2: Ddr is required for normal wrapping glia morphogenesis

(A) Model of the *Ddr* genetic locus showing the coding region (cyan); the deficiency used in experiments: *Df(2L)BSC186*; the region that the rescue BAC covers; the location of the RNAi target regions (magenta); and locations of the guide RNAs used for the CRISPR-mediated mutagenesis (magenta). **(B-D)** Representative images of Ddr RNAi knockdown with 2 independent RNAi constructs. *Nrv2-Gal4* driven tdTomato is pseudocolored green. A subset of axons is labeled with anti-Futsch antibody (magenta). Compared to control nerves **(B)**, RNAi conditions show large patches of the nerve cross section without glia membrane coverage **(C,D)**. **(E-G)** Representative images of *Ddr* homozygous mutant experiments. Compared to control **(E)** both CRISPR mutant alleles show severe defective glia coverage in the nerve cross sections **(F-G)**. **(H)** Ddr is a transmembrane receptor tyrosine kinase characterized by extracellular discoidin and discoidin-like domains and an intracellular tyrosine kinase domain. The mutant alleles generated by CRISPR-CAS9 result in a severely truncated peptide without any full domains. **(I-L)** Representative images of *Ddr* loss of function experiments. **(I)** *Nrv2-Gal4, UAS-CD8:GFP/+* was used to visualize glial morphology and is in the background of all conditions. **(J)** *Ddr^{41-2F}/DfBSC186 ("Ddr* mutant*")* nerves show incomplete coverage of the nerve cross section. This example shows a "moderate" phenotype, more examples of moderate and severe phenotypes can be seen in Supplemental Figure S2A. **(K)** Introduction of a BAC transgene to resupply endogenous *Ddr* expression largely restores normal morphology. **(L)** Expression of a *1xUAS-Ddr* construct in wrapping glia using *Nrv2-Gal4* similarly restores normal morphology. **(M)** Categorical scoring of nerve wrapping glia phenotypes. n= # of nerves scored (8-14 larvae per condition). Scale bars = 5μm.

8

128   isoforms: a short isoform that is 380 amino acids and lacks both transmembrane and kinase

129   domains, and a full-length isoform that encodes a 1054 amino acid protein. We identified two

130   independent alleles that are predicted nulls, as they result in 150 amino acid ($Ddr^{13\text{-}1M}$) or 134

131   amino acid ($Ddr^{41\text{-}2F}$) long peptides lacking all known functional domains (Figure 2H). Both

132   mutant alleles were homozygous viable and viable when placed in *trans* to large deficiencies that

133   uncover the *Ddr* coding region. We analyzed the nerves of *Ddr* homozygous mutant animals

134   using florescent confocal microscopy and found that wrapping glia morphology was impaired as

135   we had observed in the wrapping glia-specific RNAi knockdown experiments (Figure 2E-G).

136   We focused our loss of function analyses on using the combination of *Ddr$^{41\text{-}2F}$* and *Df(2L)*

137   *BSC186*, the shortest deficiency that still deletes the entire *Ddr* coding region (Figure 2A). We

138   found that animals lacking any functional Ddr had impaired wrapping (Figure 2I-J, 2M; control:

139   79% normal morphology; *Ddr/Df*: 21% normal morphology; see Figure 2—figure supplement 1

140   for examples of categorical scoring). Introduction of a single copy of a BAC clone containing

141   the entire *Ddr* locus and a ~17.4kb upstream region into the mutant strain largely restored normal

142   wrapping morphology (Figure 2K, 2M; BAC rescue: 75% normal morphology), as did

143   resupplying Ddr in wrapping glia via a *1xUAS-Ddr* construct driven by *nrv2-Gal4* (Figure 2L,

144   2M; *1xUAS* rescue: 70% normal morphology). Higher level overexpression using a *5xUAS-Ddr*

145   construct caused morphological defects in a control background that the *1xUAS-Ddr* construct

146   did not, suggesting that Ddr levels may need to be tightly regulated to promote normal wrapping

147   and morphological development (Figure 2—figure supplement 2). Together these results

148   confirmed our RNAi results that Ddr is required cell autonomously in wrapping glia to regulate

149   axon ensheathment.

150   While data from fluorescent images supported the notion that significant ensheathment

151 defects resulted from loss of Ddr, we wanted to quantify more precisely how wrapping was

152 affected in Ddr mutants. We therefore analyzed nerves from control and *Ddr* mutant animals

153 using transmission electron microscopy (TEM) and used the "wrapping index" (WI) metric to

154 quantify ensheathment defects (Matzat et al., 2015). WI is equal to the number of individually

155 wrapped axons plus the number of small bundles of axons, divided by the total number of axonal

156 profiles and is expressed as a percentage. In control condition nerves, wrapping glia membrane

157 separated axons in small bundles or individually (Figure 3A-B). The average WI in control

158 conditions was ~21% (Figure 3F: *nrv2* driver control: mean= 22.5%, n=26 nerves from 5 larvae,

159 w^{1118} control: mean= 21%, n=15 nerves from 3 larvae), consistent with previous reports (Matzat

160 et al., 2015). We observed less separation of axons by wrapping glia membrane in Ddr

161 conditions (Figure 3C-D), and this was reflected in both Ddr^{41-2F} homozygous and Ddr^{41-}

162 ^{2F}/*Df(2L)BSC186* conditions showing a significant decrease in wrapping index (Figure 3F:

163 *Ddr/Ddr* mean=14.8%, n=30 nerves from 4 larvae, p=0.0006 compared to *nrv2* control;

164 *Ddr/Df(2L)BSC186*: mean= 11.9%, n=33 nerves from 4 larvae, p<0.0001 compared to *nrv2*

165 control, one-way ANOVA with Dunnett's multiple comparisons). These data confirm that loss of

166 Ddr impairs axonal wrapping during development.

167   To determine whether loss of Ddr specifically affected wrapping glia or more grossly

168 disrupted the morphology of the nerve, we also assessed the other glial and axonal populations

169 within the nerves of Ddr mutants. We did not observe any changes in either subperineurial or

170 perineurial glia in TEM sections in the mutant conditions, nor differences in the total number of

171 axon profiles observed (Figure 3—figure supplement 1), suggesting that overall nerve assembly
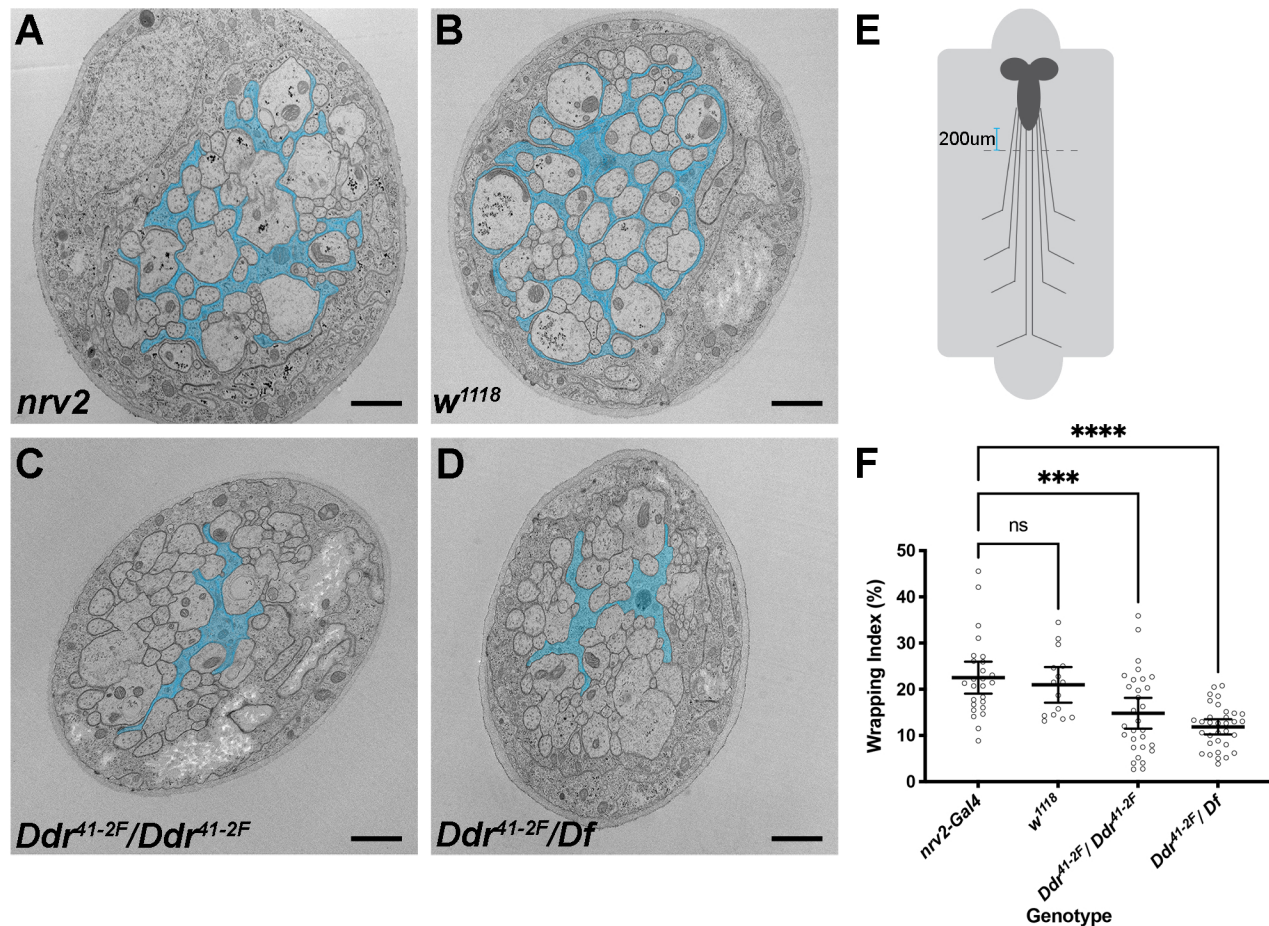
FIGURE 3

Figure 3: Loss of *Ddr* impairs axon ensheathment in larval nerves

(A) TEM cross section of an abdominal nerve from a control *nrv2-Gal4, UAS-CD8:GFP/+* 3rd instar larvae. Wrapping glia membrane is pseudocolored cyan. **(B)** TEM cross section of an abdominal nerve from a control *w^{1118}* 3rd instar larva. **(C)** TEM cross section of an abdominal nerve from a *Ddr^{41-2F}* homozygous mutant animal (*Ddr^{41-2F}/ Ddr^{41-2F}; nrv2-Gal4, UAS-CD8:GFP/+*). **(D)** TEM cross section of an abdominal nerve from a *Ddr* loss of function animal (*Ddr^{41-2F}/Df(2L)BSC186; nrv2-Gal, UAS-CD8:GFP/+*). **(E)** Schematic of larval fillets prepped for TEM. Sections for analysis are collected ~200um from the distal tip of the VNC. **(F)** Quantification using the wrapping index (WI) metric. Wrapping index was reduced in Ddr loss of function conditions compared to control conditions in larval nerves. *Nrv2-Gal4, UAS-mCD8:GFP/+* controls (WI: 22.5%, n= 26 nerves, 5 larvae); *w^{1118}* wildtype background strain (WI: 21%, n=15 nerves, 3 larvae, p=0.9546); *Ddr$^{-/-}$* (WI: 14.8%, n= 30 nerves, 4 larvae, p=0.0006); *Ddr/Df* (WI: 11.9%,n=33 nerves, 4 larvae, p<0.0001); One-way ANOVA with Dunnett's multiple comparisons against *Nrv2-Gal4*. Error bars: 95% Confidence interval. Scale bars = 1μm

11

172   was relatively normal. Therefore loss of Ddr seems to specifically alter wrapping without

173   disrupting nerve morphology.

174

175   **Incomplete ensheathment of axons is not sufficient to alter crawling behaviors**

176   We next sought to determine whether a decrease in multi-axonal ensheathment might

177   impact neuronal health and function. Larval nerves are mixed nerves that contain both the motor

178   and sensory axons that together mediate larval crawling behavior. To see if basic locomotion was

179   affected when normal axonal ensheathment was impaired, we assayed larval crawling behavior

180   in *Ddr* mutant third instar larvae by monitoring crawling on a non-nutritive agar surface using

181   the FIMTracker system (Risse et al., 2017). Comparing overall distance travelled over a one

182   minute period, we did not see any significant effects on basic crawling behavior between control

183   and *Ddr* mutant larvae (Figure 4A-B). One interpretation of these results is that wrapping is

184   completely dispensable, at least for basic crawling behaviors. Alternatively, it is possible that

185   even the incomplete wrapping observed in *Ddr* mutants is sufficient to support neuronal function

186   and this basic behavior over the ~5 day period of larval life.

187

188   **Genetic ablation of wrapping glia impairs larval crawling**

189   To further distinguish between these possibilities, we sought to ablate wrapping glia

190   entirely. These experiments required a Gal4 driver that would selectively drive expression

191   exclusively in wrapping glia. Although *Nrv2-gal4* is specific to wrapping glia in the PNS, it does

192   drive expression in some subtypes of CNS glia which would complicate the interpretation of any

193   functional ablation experiments. To generate a clean wrapping glia specific driver line, we turned

194   to a Split-Gal4 intersectional strategy (Luan et al., 2006). First, we created a *nrv2-Gal4^{DBD}*
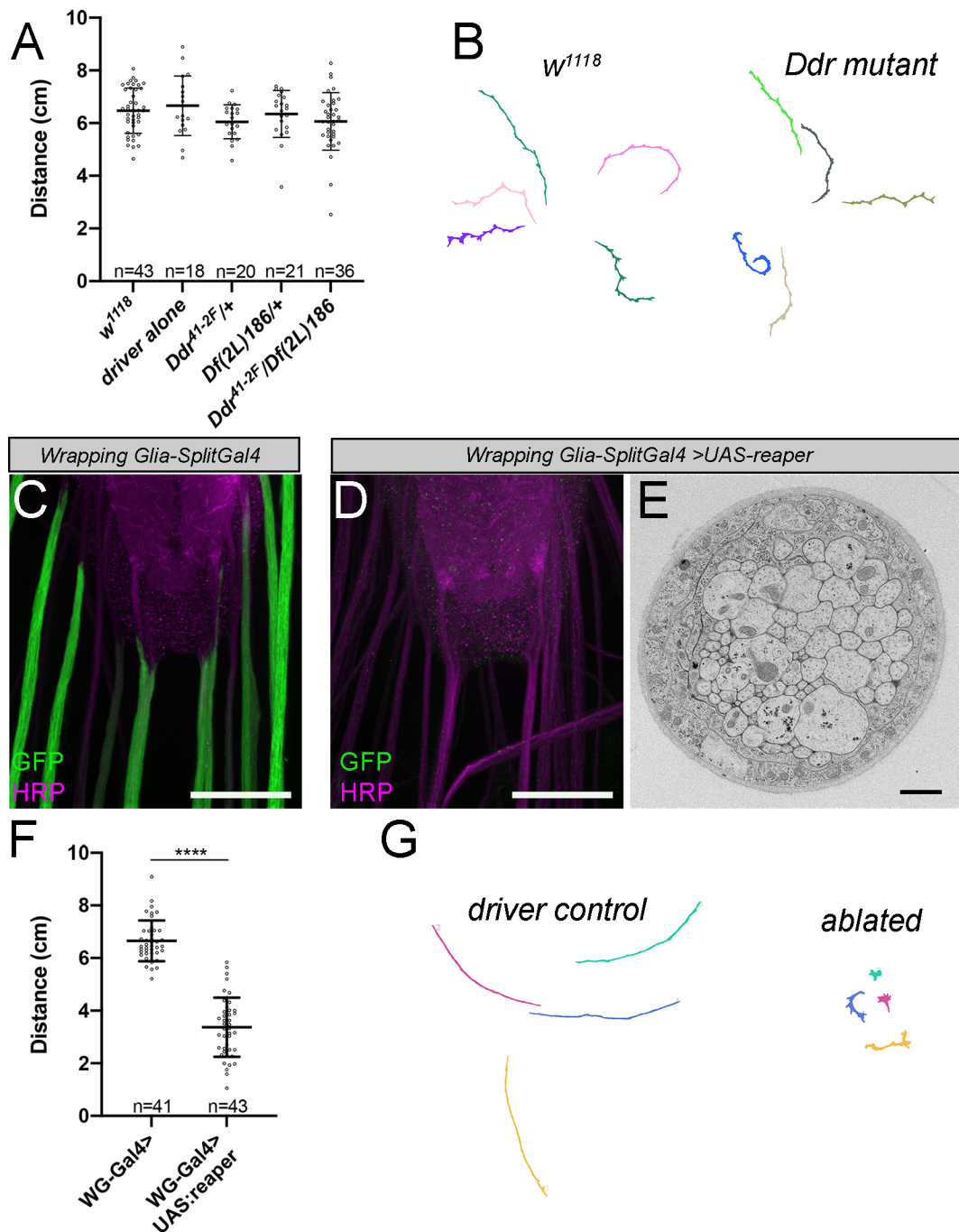
FIGURE 4

Figure 4: Genetic ablation of wrapping glia impairs larval crawling behavior.
(A) Larval crawling, as measured by distance travelled per minute is not impaired in *Ddr* mutant animals compared to control conditions. One-way ANOVA with Tukey's multiple comparisons, no significant differences between any conditions. n = # of larvae/condition. **(B)** Representative crawling paths from control and *Ddr* mutant larvae. **(C)** Expression pattern of *WG-Split-Gal4* driving *UAS-CD8:GFP* (green). Magenta is an HRP counterstain which labels neuronal membranes. Scale bar, 50μm. **(D)** Representative image of a 3rd instar larvae in which wrapping glia have been genetically ablated. Note the lack of GFP staining along the nerves. Scale bar 50μm. **(E)** TEM image of a nerve cross section from a larva whose wrapping glia has been ablated. All of the axons remain in contact with each other without intervening glial membrane. Scale bar 1μm **(F)** Larval crawling behavior is impaired when wrapping glia are ablated. Unpaired t-test, p<0.0001. n = # of larvae/condition. **(G)** Representative crawling paths of control and ablated larvae. The paths from the ablated larvae are shorter and show increased turning, stalling, and reversals. Error bars: standard deviation

13

195   construct. This line is capable of driving expression of the DNA binding domain of GAL4 in

196   wrapping glia, cortex glia, ensheathing glia, and astrocytes (Coutinho-Budd et al., 2017). We

197   then identified a line from the InSite collection (*InSite0117-Gal4*) that robustly labeled wrapping

198   glia and a subset of neurons (Figure 4—figure supplement 1). We converted *Insite0117-Gal4* to

199   *Insite0117-GAL4^{VP16AD}* line using the InSite method to swap the domains via genetic crosses

200   (Gohl et al., 2011). In conjunction with *Nrv2-Gal4^{DBD}* this results in specific expression of UAS-

201   transgenes only where the 2 hemi-drivers' expression overlaps—in wrapping glia. No other glia

202   or neurons were observed in the expression pattern (Figure 4C and Figure 4—figure supplement

203   1). This combination of *nrv2-Gal4^{DBD}* and *IT.0117-Gal4^{VP16AD}* is referred to as *wrapping glia-*

204   *Split Gal4* (*WG-SplitGal4*).

205   We used *WG-SplitGal4* to drive expression of *UAS-mCD8:GFP* and *UAS-reaper* to

206   ablate wrapping glia. We observed nearly complete loss of larval wrapping glia cells in resulting

207   progeny based on loss of both fluorescence and an independent wrapping glia nuclear marker

208   that we had identified in the lab, Oaz (Figure 4D and Figure 4—figure supplements 2 and 3).

209   To further confirm the ablation of wrapping glia, we examined the ultrastructure of nerves where

210   wrapping glia were ablated. We saw tightly fasciculated axons without intervening glial

211   membranes confirming that wrapping glia had been eliminated (Figure 4E). Only in a few nerves

212   did we identify anything that might be remnants of wrapping glia. We did not observe any

213   obvious ingrowth of the outer subperineurial or perineurial glia layers to potentially compensate

214   for the loss of wrapping glia and ensheathe axons. However, we did note that several nerves

215   showed an abnormal hypertrophy of the outer perineurial glia layer (Figure 4—figure

216   supplement 3). Surprisingly, when we counted the number of axon profiles in each nerve, we

217   found fewer axonal profiles than the expected ~78 of A3-A7 nerves (*w^{1118}* average= 77.4 axons;

218   WG-ablated average= 63 axons; Unpaired t-test p=0.0006), indicating that axons (or entire

219   neurons) might have died or not developed properly as a result of acute wrapping glia loss

220   (Figure 4—figure supplement 3).

221   Using these tools, we then assayed for defects in crawling behavior and found that

222   animals with ablated wrapping glia crawled significantly less than control animals (Figure 4F-G;

223   mean distance travelled: driver control = 6.65±0.77cm, n=41 larvae, ablated = 3.37±1.126cm,

224   n=43; p<0.0001 unpaired t-test). In performing the experiments, we also observed that larvae

225   lacking wrapping glia had difficulty righting themselves when placed on their dorsal sides, and

226   were observed to have abnormal postures and body bends, indicating a possible disruption of

227   bilateral or intersegmental coordination caused by wrapping glia ablation. Together, these data

228   demonstrate that wrapping glia are required in nerves for normal circuit function.

229

230   **Ensheathment of axons in an adult nerve is not impaired in *Ddr* mutants**

231   Unlike ablation of wrapping glia, incomplete wrapping caused by the loss of Ddr did not

232   significantly affect behavior or neuronal survival during the short larval period (~5 days).

233   However, since neuronal defects that are secondary to glial dysfunction can be age- or stress-

234   related in vertebrate animals (Beirowski et al., 2014; Lappe-Siefke et al., 2003; Saab et al., 2016;

235   Yin et al., 1998; Zöller et al., 2008), we investigated whether Ddr and proper wrapping were

236   required for longer term support of axon health and function. Because the larval period is short

237   and defined, we turned our attention to an accessible adult peripheral nerve, the L1 sensory nerve

238   in the adult wing.

239   Sensory bristles and campaniform sensilla along the wing's edge are innervated by

240   peripheral sensory neurons located within the L1 wing vein. The axons of these neurons form the

241 L1 sensory nerve that projects into the thorax (Figure 5A). The organization of the nerve is

242 reported to be similar to larval nerves, with axons ensheathed by wrapping glia (Neukomm et al.,

243 2014). We developed a protocol to perform TEM on the adult wing to examine cross sections of

244 the nerve. By imaging in the region distal to the fusing of the L3 nerve but proximal to the first

245 sensory cell body along the anterior wing margin, we could reliably visualize all of the axons

246 present in the L1 nerve (Figure 5A, dashed red box). In control nerves at 5 dpe, we were

247 surprised to find that all axons appear to be completely separated from one another (Figure 5B),

248 instead of persisting in tightly compacted small bundles as are observed in the larval nerves

249 (compare to Figure 1B). When we examined *Ddr* mutant wings of the same age, we found no

250 obvious defects in wrapping and axon separation between control and *Ddr* mutant wing nerves

251 (Figure 5C-D), in contrast to the impaired wrapping we observed in *Ddr* mutant larval nerves.

252 These data show that wrapping in the adult is more extensive than in larval nerves and seems to

253 be completed during pupal stages or shortly after eclosion. Despite being more extensive and

254 complete, wrapping in adult nerves does not strictly require Ddr. Ddr may be dispensable for

255 wrapping in the adult, work redundantly with other molecules, or cause only a transient delay in

256 wrapping that is rectified within a few days of eclosion.

257

258 Loss of Ddr impairs the long-term survival of adult sensory neurons

259   Despite having no obvious defects in axonal ensheathment, based on our observation of

260 apparent neuronal loss in wrapping glia-ablated larvae, we wondered whether long-term neuronal

261 health in the adult L1 wing nerve might be impacted by loss of Ddr from glia. To test this, we

262 labeled the ~40 glutamatergic neurons in the wing nerve using the *QF2/QUAS* binary system

263 (*VGlut-QF2; QUAS-6xGFP*)(Potter et al., 2010), while at the same time using *Repo-Gal4* to
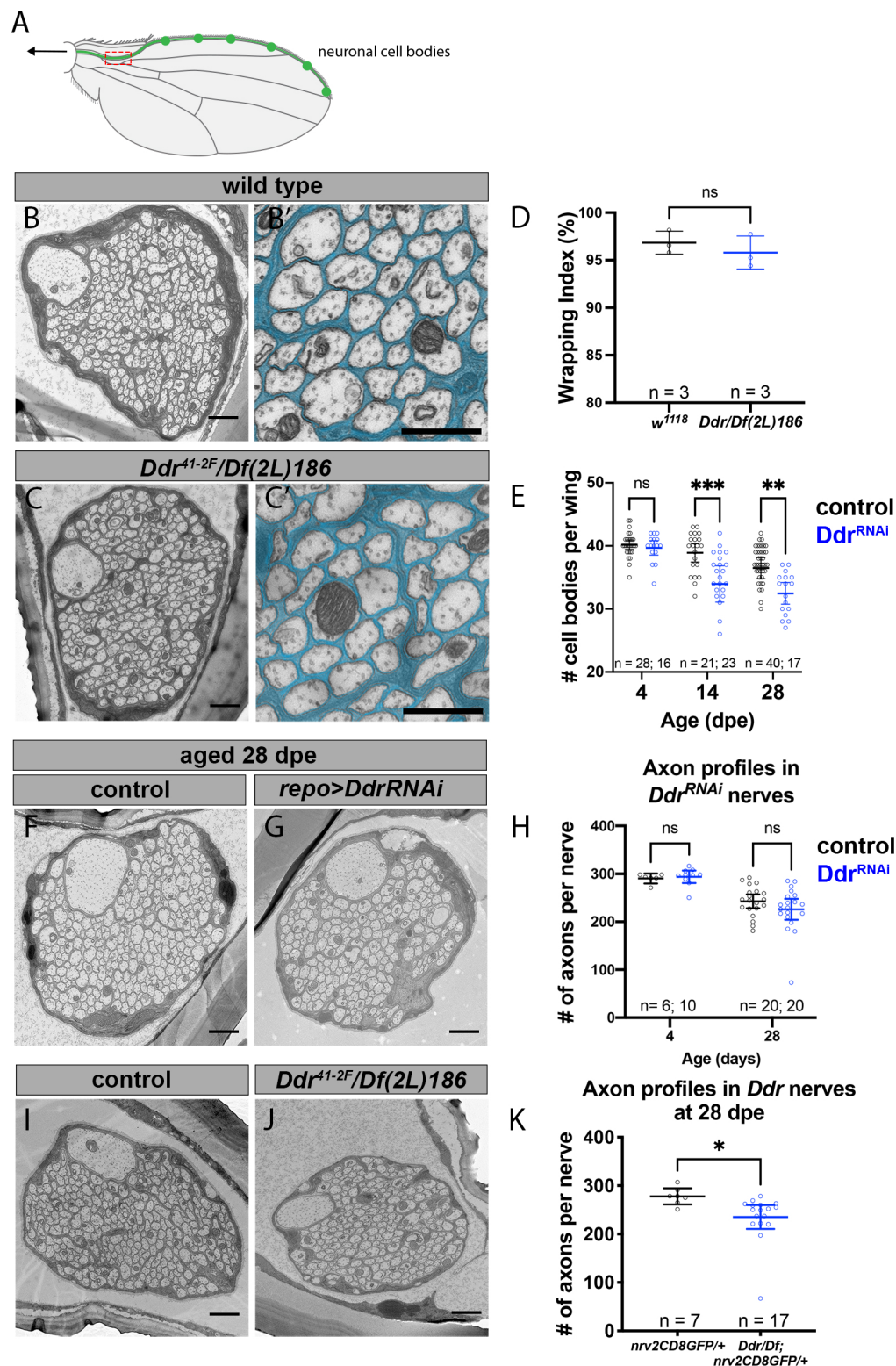
FIGURE 5

Figure 5: Loss of Ddr impairs long-term neuronal survival without affecting wrapping in adult nerves

(A) Schematic of the adult fly wing. The L1 vein lies along the anterior margin of the wing and contains ~280 sensory neuron cell bodies, a subset are depicted in green. The axons of these neurons coalesce to form the L1 sensory nerve which projects into the body towards the fly CNS. The TEM imaging window is shown in red. In this location axons from all of the L1 sensory neurons are present, allowing for quantifications. (*cont. next page*)

17

Figure 5 (cont.)
(B) Cross section TEM of the L1 nerve shows that axons are separated from each other by glial membranes by 5 dpe. (B') Magnified view from B with wrapping glia pseudocolored cyan. **(C)** Nerve morphology including wrapping is comparable in *Ddr* mutant nerves at this age, with axons separated and no obvious signs of impaired wrapping glia morphology. (C') Magnified view from C with wrapping glia pseudocolored cyan. **(D)** Wrapping index of *Ddr* loss of function animals is unchanged compared to control. (Unpaired t-test, p=0.4378) **(E)** There is a reduction in the number of healthy glutamatergic GFP+ cell bodies in wings from aged *Ddr*^{RNAi} knockdown animals compared to age-matched controls. (Two-way ANOVA with Sidak's multiple comparisons. 4dpe p=0.9774; 14dpe p=0.0007; 28dpe p=0.005) **(F)** Representative TEM image of a control nerve at 28 dpe shows normal wrapping/axon separation. **(G)** Representative *Ddr*^{RNAi} knockdown nerve at 28 dpe also shows normal wrapping/axon separation. A wrapping glia nucleus is present in this section (asterisk). **(H)** Quantification of axon profiles in 28 dpe control and *Ddr* mutant animals shows a modest but significant reduction in axons in *Ddr* as compared to controls. (Unpaired t-test, p=0.0343) **(I)** Representative TEM of a control nerve from a 28 dpe animal shows normal wrapping. **(J)** Representative TEM of a nerve from a 28 dpe *Ddr* mutant animal also shows normal wrapping. **(K)** Quantification of axon profile number in control and *Ddr*^{RNAi} glial knockdown nerves show no statistically significant difference in age dependent axon loss in contrast to our findings focusing on VGlut+ neuronal cell bodies by fluorescence (E). (Two-way ANOVA with Sidak's multiple comparisons; 4 dpe p=0.9755; 28 dpe p=0.2519)
Scale bars: B, C, F, G, I , J =1μm; B'& C' = 600nm

264   knockdown Ddr in glia using RNAi. We examined wings at 4, 14, or 28 **d**ays **p**ost **e**closion (dpe)

265   and counted healthy GFP+ neuronal cell bodies along the wing margin at these timepoints from

266   control and Ddr-RNAi animals to determine if loss of Ddr had any impact on long term neuronal

267   survival. The number of neuronal cell bodies at 4 dpe was the same between control and *Ddr*

268   knockdown animals suggesting that knockdown of *Ddr* did not affect neurogenesis (Figure 5B).

269   Despite beginning with the same number of neurons (Figure 5E: 4 dpe mean cell body count =

270   40.2 vs. 39.7, p=0.9774), we found that there were significantly fewer healthy cell bodies in aged

271   *Ddr-RNAi* wings compared to control at both ages examined (Figure 5E; 14 dpe mean cell body

272   count 38.9 vs 34.0, p=0.0007; 28 dpe mean cell body count 36.5 vs 32.5, p=0.005, 2-way

273   ANOVA with Sidak's multiple comparisons). These results indicate that despite not overtly

274   disrupting glial ensheathment, knockdown of *Ddr* in glial cells negatively impacts long-term

275   neuron health and survival.

276   To confirm and extend these findings we used TEM to visualize L1 nerves from aged

277   control and glial *Ddr-RNAi* animals. We collected cross sections from a region in which all

278   axons should be present so we could compare the total number of axon profiles within the nerve.

279   To mirror our fluorescent experiments, we used the same genotypes and we first examined wings

280   at 4 dpe. The number of axon profiles in control nerves at 4 dpe showed little variation and was

281   indistinguishable from *Ddr-RNAi* (Figure 5H: mean axon profile count 290.3±10 vs 293.9±18.3,

282   p=0.98). In aged (28 dpe) control and *Ddr* knockdown wing nerves, although wrapping again

283   appeared normal, there was overall more variability in axon profile counts (Figure 5F-H:

284   control= 242.7±31.02, *Ddr-RNAi* =226±46.5 axon profiles), but there was no significant

285   difference in axon profile count in the *Ddr-RNAi* condition (Figure 5E-G; p=0.25, 2-way

286   ANOVA with Sidak's multiple comparisons. This is in contrast to our findings in the same

287   genotype when we focused exclusively on *VGlut-QF2+* cell bodies (which marks ~40 cell bodies

288   out of ~290 cell bodies total in the L1 nerve), We repeated these experiments using *Ddr* mutant

289   animals and found a small but significant difference in the number of axon profiles (~15% fewer

290   axons) consistent with the size of our original findings with fluorescent labeling of a

291   subpopulation of these neurons (Figure 5I-K; control =277.9 ± 17.9, *Ddr* = 235.2 ± 48.2,

292   p=0.022, unpaired t-test). Since the effect was stronger in whole animal mutants, this may reflect

293   insufficient RNAi knockdown, but we cannot rule out that loss of Ddr from neurons, or another

294   tissue might contribute to this effect, or that only specific subsets of neurons are particularly

295   vulnerable to Ddr loss. Nevertheless, these data indicate that glial Ddr modulates the long-term

296   health of sensory neurons.

297

298   **Glial Ddr promotes increased axon caliber**

299   Myelination can induce many changes in underlying axons including the redistribution of

300   axonal proteins and increased axon caliber (Stassart et al., 2018), but whether non-myelinating

301   ensheathment has similar effects is not known. One striking feature of the ultrastructure of the L1

302   wing nerve was the presence of a single, prominent, large caliber axon (Figure 5B). This axon is

303   thus immediately identifiable in every sample, allowing us to directly compare its features across

304   animals and conditions. A survey of the literature revealed that this axon likely belongs to the

305   **d**istal **t**win **s**ensilla of the **m**argin (dTSM) neuron that innervates a campaniform sensillum

306   (Dickinson and Palka, 1987). A striking but unexpected observation was that the dTSM axon in

307   *Ddr* mutant and knockdown conditions was significantly smaller than in controls even though it

308   was still clearly identifiable as the largest axon in the nerve. We quantified axon caliber by

309   measuring the cross-sectional surface area of this uniquely identifiable axon and comparing
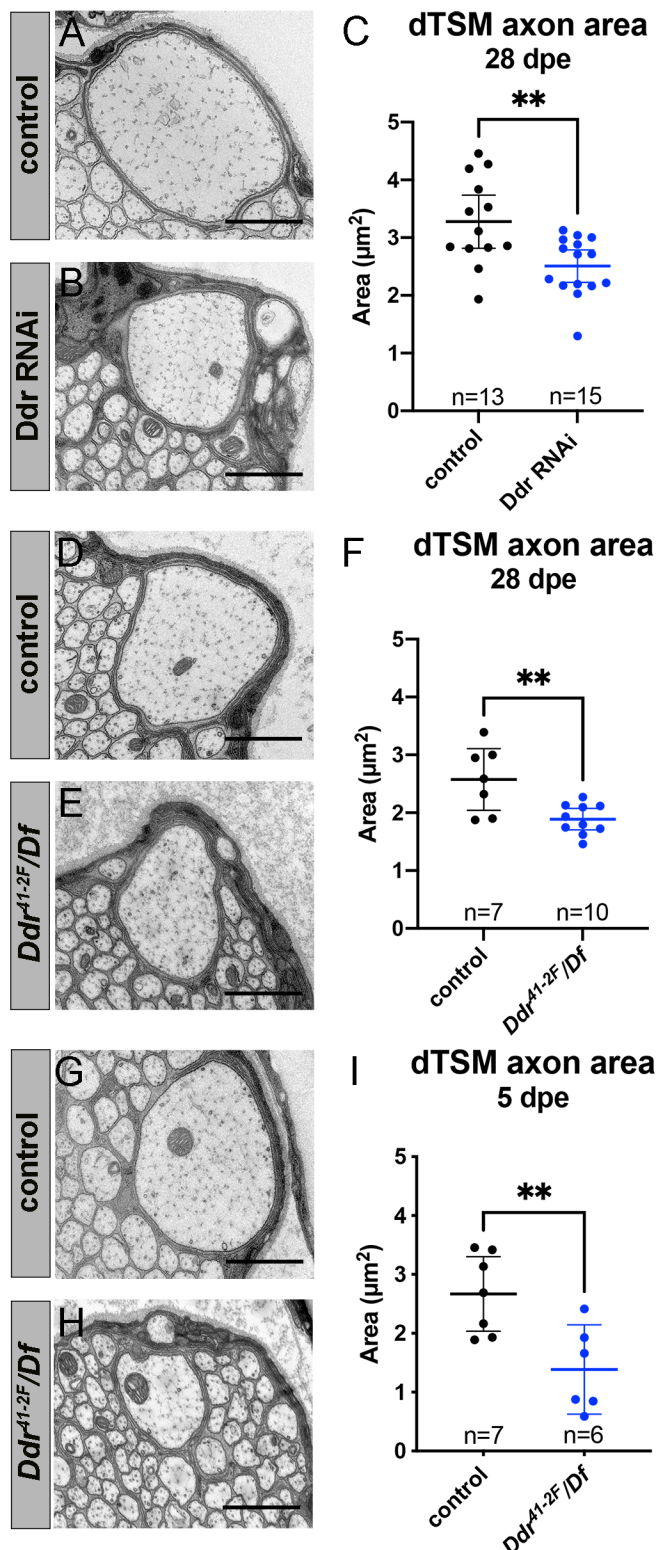
FIGURE 6

Figure 6: Ddr is required for normal axon caliber growth

(A-C) Axon caliber of the dTSM axons as measured by the cross-sectional area in TEM images is reduced in 28 dpe Ddr^{RNAi} nerves compared to age-matched controls. (Unpaired t-test; p=0.0037) **(D-F)** Axon caliber of the dTSM axons as measured by the cross sectional area in TEM images is reduced in 28 dpe *Ddr* loss of function nerves compared to age-matched controls. (Unpaired t-test; p=0.0044) **(G-I)** Axon caliber of the dTSM axons as measured by the cross sectional area in TEM images is already reduced in 5 dpe *Ddr* loss of function nerves compared to age-matched controls suggesting that initial axon maturation is perturbed when Ddr is absent. (Unpaired t-test; p=0.0073) Scale bars 1μm.

310   appropriate controls to *Ddr* mutant or glial *Ddr-RNAi* conditions from our 28 day aged wing

311   TEM images. We found that in both glial-specific *Ddr*-knockdown and *Ddr* whole animal

312   mutant nerves the caliber of the dTSM axon was significantly reduced compared to controls,

313   revealing a role for glial Ddr in modulating axonal caliber (Figure 6A-F).

314   To determine whether reduced caliber is due to reduced growth versus shrinkage, we

315   examined dTSM caliber in control and *Ddr* mutant wings from 5 dpe and found that the

316   reduction in size is even greater at this age (Figure 6G-I). dTSM axon caliber is reduced by

317   ~48% in *Ddr* mutants at 5 dpe (mean area: control = 2.670um^2 and *Ddr* = 1.387um^2) and ~27%

318   at 28 dpe (mean area control = 2.575um^2 and *Ddr* = 1.890um^2). We have examined a small

319   number of L1 nerves from wild type freshly eclosed flies (<24hours post eclosion) and observed

320   that axons appear smaller than those from our standard 5 dpe timepoint suggesting that the first

321   few days post eclosion are an important period of axon growth and maturation (Figure 6—figure

322   supplement 1). Together these data suggest that the reduced caliber we see in *Ddr* mutants is due

323   to impaired growth, rather than shrinkage. Since knockdown of Ddr selectively in glia is

324   sufficient to cause a similar reduction in caliber to what is observed in whole animal mutants

325   (~23% reduction at 28 dpe in RNAi experiments) our data identifies a cell non-autonomous role

326   for glial Ddr in the control of axon caliber.

327   The reduced neuronal survival and decreased caliber we observed led us to wonder if we

328   would observe any behavioral defects in adults as a result of Ddr loss. dTSM likely provides

329   important proprioceptive feedback during flight, but its exact role in modifying flight behavior

330   has not been established, making it difficult to directly test the effects of its reduced caliber on

331   behavior. One well-established, testable behavior in adult flies is the escape reflex mediated by

332   the giant fiber system. In this response, visual input activates the giant fiber neuron in the CNS,

22

333   which then activates an interneuron, that innervates a peripheral motor neuron to initiate a

334   jump/escape response. This circuit is extremely fast and reliable. We reasoned that if the motor

335   neuron axons in this circuit (the relevant peripheral axons in this circuit) were impaired in some

336   way, there might be a measurable decrease in the muscle response probability after stimulation

337   or an increased latency. We tested this reflex electrophysiologically in control and *Ddr* mutant

338   animals but found no significant differences between the genotypes in either young or 28 dpe

339   animals (Figure 6—figure supplement 2).

340

341   ***Ddr* interacts with *Mp* to promote wrapping in larval nerves**

342   Our data indicate that Ddr performs essential roles in wrapping glia development and

343   function. We next sought to understand the molecular mechanism(s) by which Ddr might

344   mediate these functions. Mammalian Ddrs are activated by collagens *in vitro* and are thus

345   considered non-canonical collagen receptors (Vogel et al., 1997). We wondered if *Drosophila*

346   Ddr also interacts with collagen(s) to mediate its effects on wrapping in the larvae. The

347   *Drosophila* genome contains 3 collagen genes. One of them, *Multiplexin* (*Mp*), was identified as

348   a potential hit that affected wrapping glia morphology in third instar nerves in our initial screen.

349   Knockdown of *Mp* using *nrv2-Gal4* caused moderate to severe wrapping defects when analyzed

350   by confocal microscopy (Figure 7A-B). We studied expression of Mp protein in wild type nerves

351   by using a MiMiC-GFP line in which the endogenous Mp protein is tagged with GFP. We

352   observed punctate GFP expression throughout larval nerves suggesting that Mp, a secreted

353   protein, is expressed by one or more of the cell types within the nerve (Figure 7C).

354   To determine whether *Ddr* and *Mp* might be working in the same genetic pathway to

355   modulate wrapping in larval nerves, we crossed heterozygous *Ddr* and *Mp* mutants together and
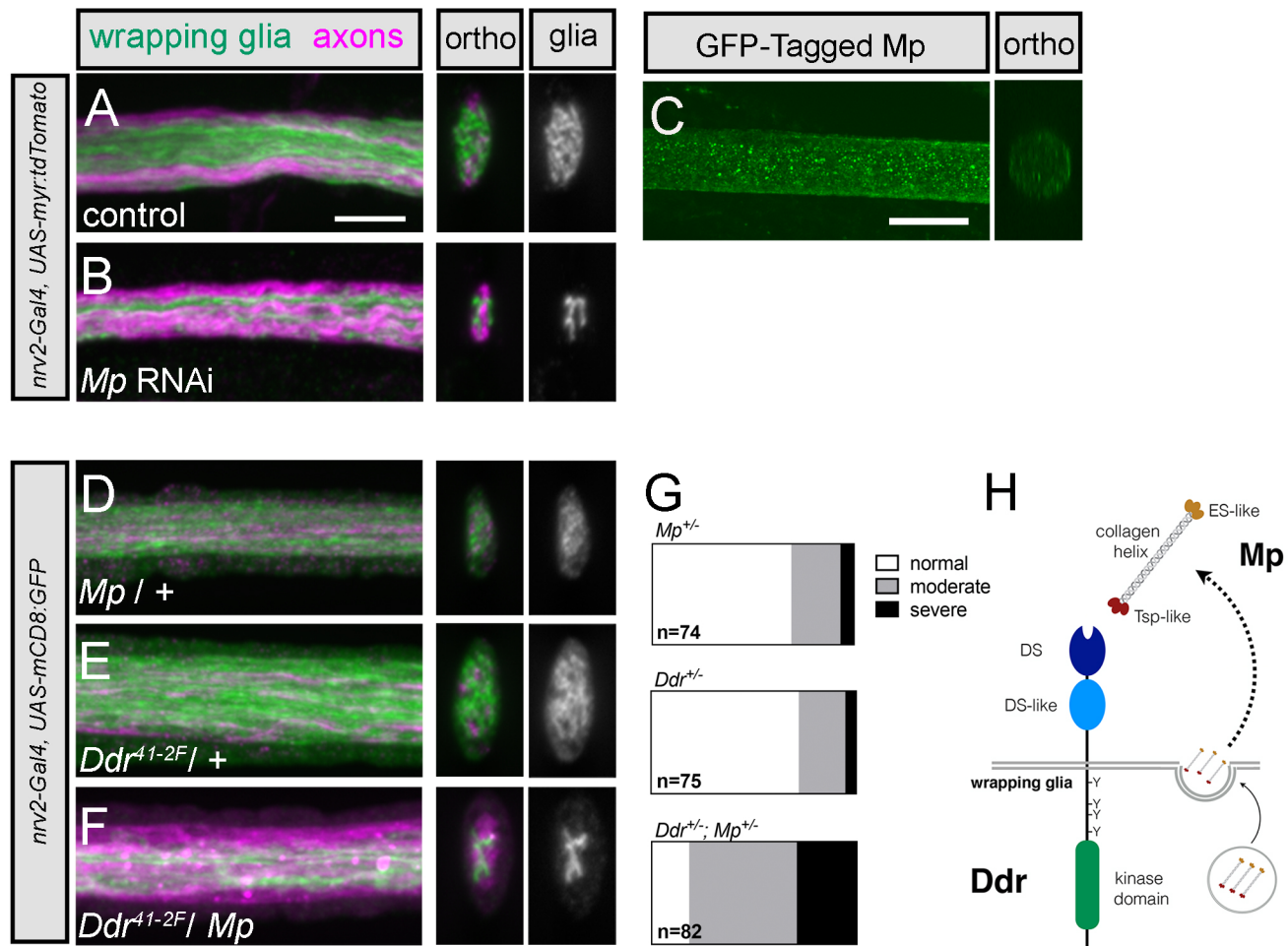
23

FIGURE 7

Figure 7: *Mp* genetically interacts with *Ddr* to promote wrapping in larval nerves

(A-B) Representative images of control and *Mp* RNAi knockdown in larval nerves. *Nrv2-Gal4* driven tdTomato is psuedocolored green. A subset of axons is labeled with anti-futsch antibody (magenta). Compared to control nerves, RNAi conditions show large areas of the nerve cross section without glia membrane coverage. **(C)** Mp-GFP expression in larval nerves. A MiMiC construct that adds a GFP tag to Mp protein is localized throughout larval nerves. **(D-F)** *Mp* and *Ddr* heterozygous nerves show normal wrapping glia morphology with good glial coverage of the nerve cross section indicating that one copy of each gene is sufficient to promote wrapping. In double heterozygous animals missing just one copy of each gene, however, coverage of the cross section is reduced indicating that wrapping is impaired. **(G)** Categorical scoring of *Ddr* and *Mp* single and double heterozygotes. n= # of nerves analyzed from 9-11 larvae per condition. **(H)** Proposed model of Mp and Ddr interaction. Based on the strong phenotype observed when Mp is knocked down specifically in wrapping glia, we hypothesize that wrapping glia secrete Mp which can act as autocrine activator of Ddr to drive normal wrapping glia morphogenesis.

24

356 analyzed the double heterozygous progeny for defects in larval wrapping glia morphology.

357 While animals that were heterozygous for either gene on its own did not show defects in

358 wrapping glia morphology, we found that the double heterozygous animals exhibited moderate

359 to severe defects in glial morphology (*Ddr/+*: 77% normal morphology; *Mp/+:* 72% normal

360 morphology; *Ddr/Mp*: 18% normal morphology; Figure 7D-G). These data suggest a strong

361 genetic interaction between the *Ddr* and *Mp* loci and imply they might function in a common

362 genetic pathway to control wrapping glia morphological development. Given that RNAi

363 knockdown of *Mp* specifically in wrapping glia is sufficient to cause a wrapping defect, our data

364 suggest a model in which Mp acts in an autocrine fashion to activate Ddr and drive downstream

365 signaling to promote wrapping (Figure 7H).

366

367 **Discussion**

368 Non-myelinating ensheathment of axons is a conserved but understudied feature of

369 peripheral nervous systems. Although this type of multi-axonal ensheathment has been less

370 studied as compared to myelination, a growing body of evidence indicates it is important for the

371 health and function of neurons and axons in the periphery. For example, Schwann cell specific

372 loss of the transmembrane receptor LDL receptor related protein-1 (LRP1) causes both thin

373 myelin and abnormal Remak bundle structure. These cKO animals also showed a lowered pain

374 threshold, suggesting that the physiology of nociceptor neurons is impaired when Remak

375 ensheathment is disrupted (Orita et al., 2013). Disrupting metabolism in SCs causes progressive

376 axon loss, with small unmyelinated fibers dying first, before myelinated fibers begin to show

377 signs of degeneration (Beirowski et al., 2014; Viader et al., 2013, 2011). In the fly, disruption of

378 axonal wrapping leads to uncoordinated behavioral responses that hint at aberrant ephaptic

379   coupling between neighboring axons in nerves when not properly separated (Kottmeier et al.,

380   2020). Such coupling could cause inappropriate activation of sensory or nociceptive neurons

381   underlying peripheral neuropathies. Previous studies from our lab have shown that wrapping glia

382   are required to clear neuronal debris after nerve injury and mediate injury signaling between

383   injured and intact "bystander" neurons which might be important for functional recovery after

384   nerve trauma (Hsu et al., 2021; Neukomm et al., 2014). These and other findings suggest that

385   Remak-type ensheathment and axon-glia signaling of unmyelinated fibers plays a variety of

386   underappreciated roles in peripheral nerve physiology that contribute to the pathophysiology of a

387   number of PNS disorders including debilitating peripheral neuropathies and responses to nerve

388   injury.

389   In order to gain insight into non-myelinating ensheathment, we used the *Drosophila*

390   peripheral nerves to identify a novel molecular pathway important for the development and

391   function multi-axonal ensheathment. We generated a new Split-Gal4 intersectional driver to

392   specifically target wrapping glia for functional and behavioral studies to better understand how

393   wrapping glia support axon health, physiology and ultimately circuit function. Finally, we

394   uncovered roles for glia in mediating long-term neuronal survival and driving increased axon

395   caliber that are separable from overt effects on wrapping, demonstrating that non-myelinating

396   ensheathing glia perform critical, previously unappreciated, roles in nervous system

397   development, maintenance, and function.

398

399   *Ddr and Mp regulate wrapping in larval nerves*

400   A main advantage of *Drosophila* is the ability to conduct large scale *in vivo* screens. We

401   made use of available *UAS-RNAi* libraries to broadly screen for novel regulators of axonal

402 ensheathment in intact nerves. Our morphological screen was sensitive enough to identify genes

403 previously implicated in wrapping glia development including *vn*, *LamB1*, and *mys*, validating

404 our approach. Moreover, in the case of *Ddr*, we were able to identify an important novel

405 regulator of ensheathment that a simple behavioral or lethality screen would have missed in light

406 of our follow-up behavioral testing. Knockdown of *Ddr* specifically in wrapping glia resulted in

407 reduced glial membrane coverage in nerve cross sections by fluorescence microscopy. Similar

408 phenotypes were observed in *Ddr* loss-of-function animals and could be rescued by resupplying

409 Ddr specifically in wrapping glia, confirming the specificity of our RNAi results. TEM clearly

410 showed that reduced glial membrane coverage at the light level corresponds to decreased axon

411 wrapping. Unexpectedly, we observed that strong overexpression of *Ddr* using a *5XUAS-Ddr*

412 construct in a control background caused frequent morphological defects in wrapping glia that

413 were not observed when using a *1XUAS-Ddr* construct, suggesting that Ddr signaling must be

414 tightly regulated to successfully promote wrapping.

415   Though neither of the vertebrate homologs, Ddr1 or Ddr2 has been explicitly implicated

416 in glial development, several lines of evidence suggests that Ddr1 may have a conserved role in

417 vertebrate glial development or function. Ddr1 is highly expressed in the mouse OL lineage

418 starting from when the cells begin to associate with axons, is upregulated in newly formed OLs

419 after cuprizone treatment, and is expressed in both myelinating and Remak Schwann cells

420 (Franco-Pons et al., 2009, 2006; Gerber et al., 2021; Zhang et al., 2014). Moreover, Ddr1 is

421 expressed in human oligodendrocytes and myelin, and variants in the human gene have been

422 correlated with abnormal white matter and schizophrenia (Gas et al., 2018; Roig et al., 2010).

423   Vertebrate Ddr1 and Ddr2 are potently activated by collagens in vitro (Vogel et al.,

424 1997), prompting us to investigate whether collagens were involved with Ddr function in fly

425 nerves. We had discovered that loss of the *Drosophila* collagen Mp disrupted glial morphology

426 in our initial RNAi screening, and so investigated whether these genes might work together to

427 promote ensheathment. Together with mammalian Ddrs established roles as collagen receptors,

428 the strong genetic interaction we observed between *Ddr* and *Mp* is consistent with a model in

429 which Mp acts as a collagen ligand for Ddr during axonal ensheathment. Our expression data

430 from the *Mp-GFP* protein trap showed expression throughout the nerve. Although previous

431 reports indicate that Mp is also expressed in one or both of the outer peripheral glia layers that

432 extend beyond the nerve to cover NMJ synapses (Wang et al., 2019), the strong ensheathment

433 defect seen when *Mp* is knocked down exclusively in wrapping glia indicates that wrapping glia

434 themselves are the primary source of the Mp required for wrapping glia morphogenesis.

435   We hypothesize that Mp can act an autocrine collagen ligand to activate glial Ddr to drive

436 wrapping in larval nerves (Figure 7H). This parallels developing Schwann cells, which secrete

437 their own basal lamina, several components of which acts as regulators of their development

438 including laminins and collagen. For example, laminin-211 serves as a ligand for GPR126 to

439 promote myelination (Petersen et al., 2015). Mp is the sole *Drosophila* homolog of collagen

440 types XV/XVIII, containing a central helical collagen region with a cleavable N-terminus

441 thrombospondin like domain and C-terminal endostatin like domain (Meyer and Moussian, 2009;

442 Myllyharju and Kivirikko, 2004). Collagen 15a1 and 18a1 are expressed in mouse peripheral

443 nerves and *col15a1* mutants have radial sorting defects, suggesting that *Mp*'s role in promoting

444 axon wrapping is likely conserved (Chen et al., 2015; Gerber et al., 2021; Rasi et al., 2010). In

445 fact, *Mp* appears to play multiple important roles in nerve biology. Mp secreted by the outer glia

446 layers acts via its cleaved endostatin domain, which is essential for homeostatic plasticity at

447 motor neuron synapses (Wang et al., 2019, 2014). How Ddr activation within wrapping glia

28

448   ultimately drives axon wrapping still remains to be determined, but Ddr joins two other RTKs—

449   EGFR and FGFR—as important and conserved regulators of axon ensheathment (Franzdóttir et

450   al., 2009; Kottmeier et al., 2020; Matzat et al., 2015).

451

452   *Wrapping glia are required for normal larval behavior*

453   The *nrv2-Gal4* driver has been the standard method to genetically target wrapping glia in

454   the field for many years but is imperfect for manipulation of wrapping glia in ablation or

455   behavioral assays due to its expression in several subtypes of CNS glia. We generated a new

456   Split-Gal4 intersectional driver that drives exclusively in wrapping glia. This allowed us to

457   perform precise wrapping glia ablation. We found that genetic ablation of wrapping glia led to

458   severely impaired larval locomotion, indicating the wrapping glia are essential for basic crawling

459   circuit function. This phenotype was particularly striking in light of that fact that we did not

460   observe any clear crawling defect in *Ddr* mutant larvae, even though wrapping was severely

461   impaired. There are several possible explanations for these observations. First, it may be possible

462   that non-contact mediated mechanisms, such as one or more secreted factors constitute wrapping

463   glia's essential contribution to axon health and physiology. Alternatively, perhaps even a small

464   amount of direct glia-axon contact at any point along the axon length may be sufficient to

465   support axon function. This would be consistent with the lack of overt behavioral defects in

466   newly-hatched 1st instar larvae, which have poor wrapping compared to later stages (Matzat et

467   al., 2015; Stork et al., 2008), and even in wild type third instar larvae, in which not every axon is

468   individually wrapped. This supports the notion that at least in the larvae, wrapping per se may

469   not be strictly required, but glial presence and/or metabolic support and perhaps at least some

470   contact is sufficient to support function for the ~5 days of larval life. Our results are similar to

29

471   what has been recently reported (Kottmeier et al., 2020) using a different approach to target

472   wrapping glia for ablation, where only minor behavioral defects were observed when disrupting

473   the FGFR signaling but profound crawling defects were seen upon ablation. Together these data

474   support the conclusion that even limited wrapping or simply some degree of glia-axon contact is

475   sufficient to support axon survival and nerve function compared to no glia at all.

476

477   *Loss of Ddr impairs long-term neuronal survival*

478   To better study the long-term functional effects of Ddr loss in wrapping glia, we turned to

479   an adult nerve. Previous studies of oligodendrocytes and Schwann cells have found that

480   impairing glial function can result in seemingly normal wrapping and circuit function in young

481   animals, with deficits only appearing when the system is stressed or aged (Beirowski et al., 2014;

482   Lappe-Siefke et al., 2003; Saab et al., 2016; Zöller et al., 2008), and studying wrapping in the

483   adult allows for aging and maintenance studies that the short larval period precludes. Adult

484   peripheral nerves are encased in a transparent but hard cuticle that allows for live-imaging but

485   makes fixation challenging. Because of the resolution limits of light microscopy, we established

486   a reliable method to study their ultrastructure using TEM. We found that the wrapping of axons

487   by glia in the adult wing nerve is strikingly different from the larva, as all axons appear to be

488   separated and individually ensheathed by glial membranes. To our surprise, wrapping was not

489   obviously impaired in adult nerves of *Ddr* knockdown or mutant animals. Whether this is

490   because it causes only a transient delay during pupal development, or is simply not required for

491   adult wrapping glia morphogenesis remains unclear. In larval wrapping glia, there are 3 RTKs

492   (EGFR, the FGFR heartless, and now Ddr) that are each required for normal ensheathment, and

493   thus cannot fully compensate for one another (Kottmeier et al., 2020; Matzat et al., 2015). One

494   difference between larval and adult wrapping glia is the size of each cell. One larval wrapping

495   glia cell covers the majority of the nerve length from where it exits the VNC to the territory of

496   the second wrapping glia which has its cell body where nerve enters the muscle field. This means

497   that the wrapping glia cell must undergo tremendous growth to both keep up with longitudinal

498   growth as the animal grows and elongates the nerve, as well as radial growth to separate axons.

499   A single cell can end up covering from ~750um-2.5mm of nerve length depending on the

500   segment. In the wing nerve, there are ~15 wrapping glia along the region of the L1 nerve we

501   analyze, which is ~400um long. Perhaps in the larval system the cell is pushed to its growth

502   limits and any perturbation in pro-wrapping signaling has a strong effect of morphology, whereas

503   in the adult nerve the system is robust and redundant enough to withstand perturbations of single

504   genes.

505   Despite no obvious wrapping effect, however, we found that loss of *Ddr* did affect the

506   sensory neurons in the nerve as animals naturally aged. The uncoupling of neuron health from

507   overt effects on myelination has been demonstrated previously. For example, *Cnp1* mutant mice

508   show severe age-dependent neurodegeneration although they have grossly normal myelin with

509   only subtle changes in myelin ultrastructure revealed by special fixation techniques (Lappe-

510   Siefke et al., 2003; Snaidero et al., 2017). Similarly, loss of PLP results in axon degeneration

511   despite having normal myelin with only subtle ultrastructural defects (Garbern et al., 2002;

512   Griffiths et al., 1998; Klugmann et al., 1997). We found that the number of VGlut+ neurons was

513   reduced in aged wings of *Ddr* knock down animals, indicating that glial *Ddr* is important for

514   long-term neuronal survival. When we analyzed *Ddr* whole animal mutants by TEM we found a

515   small but significant reduction in axon profile number, which should correspond to the number

516   of living neurons. The effects were modest, and together with the increased variability observed

31

517   suggests to us that absence of Ddr signaling increases the susceptibility of subpopulations of

518   neurons to insult or injury that may underlie age-related degeneration rather than outright

519   causing them to die. While we cannot rule out the possibility that loss of Ddr from neurons or

520   epithelial cells contributes to the effect we see in the whole animal mutant experiments, taken

521   together our data support a role for Ddr in mediating axon-glia signaling that contributes to the

522   long-term health of peripheral neurons.

523

524   *Glial Ddr regulates axon caliber*

525   Myelination can directly affect the structure and function of the axons they wrap,

526   including controlling caliber. In general, myelination increases caliber. For example,

527   dysmyelinated *Trembler* mice have reduced axon calibers compared to controls (Waegh et al.,

528   1992) and in the PNS caliber along a single axon can vary with reduced caliber at points without

529   direct myelin contact, such as nodes of Ranvier (Hsieh et al., 1994). Axon caliber is an important

530   determinant of conduction velocity but varies widely between neuronal subtypes, so achieving

531   and maintaining appropriate caliber for each axon during development is likely to be critical for

532   proper circuit function. How non-myelinating ensheathment might impact axon caliber has not

533   been as clearly established. Here, we find that glial Ddr promotes increased axon caliber of a

534   non-myelinated axon. We focused on the dTSM axon, which can be reliably identified across

535   animals, so we could directly compare caliber between conditions. The reductions we observed

536   in axon caliber were similar between *Ddr* mutants and when Ddr was specifically lost from glia

537   cells, supporting a non-cell autonomous role for glial Ddr in regulating axon caliber. The effect

538   is considerable—nearly a 50% reduction in axon caliber at 5 dpe. We hypothesize that by this

539   time point, wildtype dTSM axons have reached their mature caliber, as it is comparable between

540   5 dpe and 28 dpe in comparable genetic backgrounds. In *Ddr* mutants, however, we observe that

541   the relative size compared to controls changes over time, suggesting that in *Ddr* mutants (or

542   knockdowns) the axon continues to increase its caliber, perhaps in an effort to achieve the

543   optimal size, though the axons still remain ~25% smaller than wild type axons at 28 dpe.

544   Two proteins, MAG, which acts to increase caliber of myelinated axons (Yin et al.,

545   1998), and CMTM6, which restricts caliber of myelinated and unmyelinated axons (Eichel et al.,

546   2020) are the only proteins reported to cell non-autonomously affect caliber of vertebrate axons.

547   In the fly, a shift in the average size of axons in larval nerves is observed when wrapping glia are

548   absent or severely disrupted supporting a general role for wrapping in promoting axon size

549   (Kottmeier et al., 2020). Interestingly, we show that Ddr is required for increased axon caliber

550   even when wrapping appears intact supporting a direct role for glial Ddr in promoting increased

551   caliber. The exact molecular mechanism by which Ddr may promote increased caliber size

552   remains unclear. The control of axon caliber, generally, is not well understood, with few studies

553   looking at either cell autonomous or non-autonomous control of caliber. Genes involved in the

554   general regulation of cell size have been implicated as cell autonomous determinants. For

555   example, in the fly, S6 kinase signaling is a positive regulator of motorneuron size, including

556   axon caliber, though the exact mechanisms that determine final caliber remain unknown (Cheng

557   et al., 2011). In mammalian axons, it is believed that the phosphorylation state of neurofilaments

558   and microtubules ultimately determines their spacing to control caliber (Yin et al., 1998). It

559   seems unlikely that *glial* Ddr can directly phosphorylate *axonal* microtubules, so determining

560   how Ddr activity in glia influences the axonal cytoskeleton to control caliber growth is an

561   important next step. Our giant fiber assay did not reveal any clear deficits in escape reflex

562   circuitry, but this circuitry mediates an extremely robust all-or-none escape response that does

563   not depend on proprioceptive feedback along long peripherally wrapped axons. A 25-50%

564   reduction in caliber would be predicted to impact conduction velocity along the dTSM axon and

565   given that campaniform sensilla provide essential rapid sensory feedback to fine tune movement,

566   it will be of interest to test conduction velocity and/or flight behavior directly in *Ddr* mutant

567   animals to see how the proprioceptive circuit might be affected.

568   Taken together, our studies identify Ddr an an important regulator of wrapping glia

569   development and function in the fly, with distinct roles in larval and adult wrapping glia. Ddr is

570   essential for the normal morphological development of axon wrapping in the larvae, and later it

571   mediates important axon-glia communication that controls axon caliber growth and affects

572   neuronal health and survival. Given its expression pattern in vertebrate oligodendrocytes and

573   Schwann cells, it seems likely that one or more of these essential functions is conserved in

574   vertebrates. Further study into how Ddr functions in both fly and vertebrate glia promises to

575   increase our understanding of axon ensheathment in health and disease.

576

577   **Methods**

578   ***Drosophila* genetics**

579   *Drosophila melanogaster* were raised according to standard laboratory conditions. Larval

580   RNAi experiments, including controls, were conducted at 29°C to increase expression of the

581   UAS-RNAi constructs. All other experimental crosses and aging experiments were conducted at

582   25°C. A full list of all fly strains used in this study can be found as a table in the Supplemental

583   Methods. Fly strains generated for this study include *Ddr*$^{41-2F}$, *Ddr*$^{13-1M}$, *WG-SplitGal4, 5XUAS-*

584   *Ddr* and *1XUAS-Ddr*. Full details on their construction are also in the Supplemental Methods.

585

Immunohistochemistry and Confocal Analysis

587   For confocal fluorescent imaging, larvae were filleted on sylgard plates in room

588   temperature (RT) PBS and fixed on a shaker in 4% paraformaldehyde (Electron Microscopy

589   Sciences, EMS) in PBS for 20 minutes. After washing with PBS and PBST (0.3% Triton-X),

590   larvae were incubated in primary antibodies overnight at 4°C with gentle agitation on a shaker.

591   After washing in PBST at RT on a shaker, secondary antibodies were added and incubated

592   overnight at 4°C on a shaker, shielded from light. After washes in PBST, samples were mounted

593   on glass slides using Vectashield (Vector Labs). The following primary antibodies were used in

594   this study: chicken α-GFP (1:1000, Abcam, ab13970); rabbit α-DsRed (1:600, Clontech,

595   #632496); rat α-mCherry (1:2000, Invitrogen, #16D7); mouse α-futsch (22C10, 1:500, DSHB);

596   mouse α-Repo (1:100, DSHB); goat α-HRP pre-conjugated to Alexa488, CY3, or CY5 (1:100,

597   Jackson Immuno Research); rabbit α-Oaz (1:5000, this study, see details below). Primary

598   antibodies were detected with the appropriate donkey secondary antibody conjugated to DyLight

599   488, Alexa488, Cy3, Rhodamine Red-X, CY5, or DyLight 405 reconstituted per the

600   manufacturer's instructions and use at final dilutions of 1:250 (Jackson Immuno Research).

601   Phalloidin-iFluor 647 and 405 were used at 1:2500 (Abcam).

602   Confocal images were obtained on either an Innovative Imaging Innovations (3i)

603   spinning-disk confocal microscope equipped with a Yokogawa CSX-X1 scan head and

604   Hamamatsu camera with SlideBook software (3i) or on a Zeiss spinning disk confocal

605   microscope equipped with a Yokogawa CSX-X1 scan head and Hamamatsu camera with Zen

35

606   software. Images were obtained with 10x air, 40x 1.3NA Oil, or 63x 1.4NA Oil objectives.

607   Confocal stacks taken to analyze wrapping glia morphology in nerve cross sections were taken

608   with the 63x objective, using the recommended optimal slice size of 0.27 microns.

609   To score wrapping glia morphology, images were obtained from regions ~200 microns

610   from the tip of the VNC (to roughly correspond to the TEM analysis location). At 63x

611   magnification ~100um of nerve length could be analyzed in an image. Orthogonal sections were

612   visualized using SlideBook or Zen software and the cross section of each nerve was examined

613   over the length in the captured image. Morphology was scored categorically as being "normal,"

614   having "moderate" defects in nerve coverage, or having "severe" defects in nerve coverage.

615   Nerves were not scored if the Z axis of a particular nerve was too compressed to visualize

616   morphology well. Representative orthogonal views were exported to prepare figures. See Figure

617   2—figure supplement 1 for images and descriptions of each category. The number of larvae and

618   nerves scored for each quantified genotype is included in the text or appropriate Figure legend.

619

620   **Electron microscopy**

621   Third instar larvae were manually processed for TEM as dissected fillets, using standard

622   TEM processing procedures. Drosophila wings were processed using microwave-assisted

623   fixation with a protocol adapted from (Cunningham and Monk, 2018; Czopka and Lyons, 2011)

624   protocols for zebrafish larvae, with the main differences being the elimination of all 10 minute

625   RT "hold" steps. After fixation and embedding in Embed-812, 70nm sections were collected on

626   200 mesh copper grids (larvae) or 100 mesh Formvar film coated grids (wings), counterstained

627   with UA and lead citrate and imaged on a Tecnai T12 electron microscope operating at 80kV or

628   120kV accelerating voltage equipped with an AMT digital camera and software. Full details of

629   fixation and processing are available in the Supplemental Methods.

630

631   **Aging assay and live imaging of wings**

632   Animals of appropriate genotypes were crossed at 25°C. Correct progeny were selected

633   using visible markers and aged in small groups in cornmeal agar vials for the indicated number

634   of days at 25°C. Flies were transferred to fresh food vials every 3-7 days. On the appropriate day

635   (4, 14, or 28 days after collection), flies were anesthetized and one wing was removed from each

636   animal using fine dissection scissors (Fine Science Tools). Wings used for fluorescence imaging

637   were mounted in Halocarbon oil 27 (Sigma) on glass slides for live imaging as described in

638   (Neukomm et al., 2014). For the neuronal survival assay, wings were inspected for tears and

639   injuries along the L1 vein at 63x with transmitted light and only wings with no visible physical

640   damage were assessed further. GFP+ cell bodies were visualized and counted using a Zeiss

641   Spinning Disk confocal system (Axio Examiner equipped with a Yokogawa spinning disk,

642   Hamatsu camera, and Zen software) using a 63xNA1.4 oil objective. Cells were counted as intact

643   if they had a clear nucleus and dendrite or were considered dead if they were shrunken and the

644   dendrite or nucleus were not clearly visible. Wings to be analyzed by TEM were immediately

645   placed in fixative and processed as described in the Supplemental Methods.

646

647   **Larval Tracking**

648   Larval crawling behavior was analyzed using the frustrated total internal reflection imaging

649   method and FIMTrack software (Risse et al., 2017). Briefly, larvae were washed briefly in

650   ddH20 and kept on agar plates prior to testing. Approximately 5 larvae of the same genotype

651   were placed near the center of a 0.8% agar surface positioned above an IR camera using a

652   paintbrush. Behavior was recorded at RT at 10 frames/second for 1 minute. Videos were

653   analyzed using FIMTrack software to extract data about individual larva. Crawling paths for

654   each larva were automatically generated by FIMTrack and information of total distance travelled

655   for each larva was exported to Excel and converted from pixels to cm before being analyzed

656   using GraphPad PRISM software. Only larvae that were successfully tracked for the full minute

657   were included in the analysis.

658

659   **Giant Fiber Assay**

660   This assay was performed essentially as described in (Allen and Godenschwege, 2010).

661   Flies of the appropriate genotype and age are mounted ventral side down under a microscope.

662   Stimulating electrodes were placed through the eyes to the brain and a recording electrode was

663   placed in the DLM muscle. 100 or 200 Hz stimulation trains were applied and responses were

664   recorded in the DLM muscle. The number of responses and the latency of the first response were

665   quantified. Data were analyzed with the GraphPad Prism, using either Mann-Whitney's test (for

666   non-parametric data) or Welch's t-test (for parametric data) to determine statistical differences.

667

668   **Analysis and Statistics**

669   TEM image analysis was performed in FIJI/ImageJ using an AMT plugin to import

670   image metadata. Wrapping index (WI) was quantified as described in Matzat et al, 2015.

671   Briefly, the Cell Counter plugin was used to manually tally the total number of axons and then

672   manually tally the number of bundles or singly wrapped axons. WI was then computed for each

673   nerve as: # of singly wrapped + # axon bundles/Total # of axons, expressed as a percentage.

674 Axon counts in wing nerves were also performed manually with the Cell Counter plugin in FIJI.

675 dTSM cross sectional area was performed using the polygon selection tool to manually trace the

676 circumference of the dTSM axon and then using the Measure Tool to obtain the cross-sectional

677 area that had been outlined. Nerves were excluded from an analysis if knife marks, resin folds, or

678 debris blocked the feature(s) needing to be measured or if the section angle was too far from

679 perpendicular resulting in elongated and blurry axonal profiles. For larval experiments, both

680 male and female larvae were used unless the genetics of a specific experiment only allowed for

681 one sex to be used (e.g. transgene on the X chromosome coming from a male parent). For adult

682 experiments only female flies (wings) were used. Wing size and the number and type of sensory

683 neruons present in the wing are sexually dimorphic, which necessitated using a single sex to

684 compare axon number and caliber. Females were selected because their wings are slightly larger

685 and thus easier to handle, and this facilitates genetic experiments that involve genes and/or

686 transgenes on the X chromosome.

687 Statistical analysis was performed using GraphPad Prism software. The appropriate

688 statistical test was determined based on the experimental design and how many conditions were

689 being compared. Details on the exact sample sizes and statistical tests used are included in the

690 corresponding Results section and/or Figure.

691

692

693

694
695 Author Contributions:
696
697 M.M.C.: Conceptualization, Methodology, Formal Analysis, Investigation, Data Curation,
698 Writing-Original Draft, Visualization, Project Administration, Funding Acquisition

699   A.P.L.: Methodology, Formal Analysis, Investigation, Data curation, Writing-Review and
700   Editing, Visualization
701   J.Q.H.: Methodology, Investigation, Writing-Review and editing
702   A.E.S.: Investigation
703   F.J.B-G.: Investigation, Formal Analysis, Writing-Review and Editing, Visualization
704   G. W.D.: Resources, Writing-Review and Editing, Funding Acquistion
705   S.A.A.: Resources, Writing-Review and Editing, Funding Acquisition
706   M.R.F.: Conceptualization, Resources, Generation of the anti-Oaz antibody, Writing-Review and
707   Editing, Project Administration, Supervision, Funding Acquisition
708

709   Acknowledgements

729   References

730
731

732   Allen MJ, Godenschwege TA. 2010. Electrophysiological Recordings from the Drosophila Giant
733   Fiber System (GFS). *Cold Spring Harb Protoc* 2010:pdb.prot5453. doi:10.1101/pdb.prot5453

734   Barros CS, Nguyen T, Spencer KSR, Nishiyama A, Colognato H, Müller U. 2009. Beta1
735   integrins are required for normal CNS myelination and promote AKT-dependent myelin
736   outgrowth. *Development (Cambridge, England)* 136:2717–2724. doi:10.1242/dev.038679

737   Beirowski B, Babetto E, Golden JP, Chen Y-J, Yang K, Gross RW, Patti GJ, Milbrandt J. 2014.
738   Metabolic regulator LKB1 is crucial for Schwann cell-mediated axon maintenance. *Nature*
739   *neuroscience* 1–15. doi:10.1038/nn.3809

740   Chen P, Cescon M, Bonaldo P. 2015. The Role of Collagens in Peripheral Nerve Myelination
741   and Function. *Molecular neurobiology* 52:216–225. doi:10.1007/s12035-014-8862-y

742   Cheng L, Locke C, Davis GW. 2011. S6 kinase localizes to the presynaptic active zone and
743   functions with PDK1 to control synapse development. *J Cell Biology* 194:921–935.
744   doi:10.1083/jcb.201101042

745   Coutinho-Budd JC, Sheehan AE, Freeman MR. 2017. The secreted neurotrophin Spätzle 3
746   promotes glial morphogenesis and supports neuronal survival and function. *Gene Dev*
747   31:2023–2038. doi:10.1101/gad.305888.117

748   Cunningham RL, Monk KR. 2018. Schwann Cells, Methods and Protocols 385–400.
749   doi:10.1007/978-1-4939-7649-2_26

750   Czopka T, Lyons DA. 2011. Chapter 2 Dissecting Mechanisms of Myelinated Axon Formation
751   Using Zebrafish. *Methods Cell Biol* 105:25–62. doi:10.1016/b978-0-12-381320-6.00002-3

752   Dickinson M, Palka J. 1987. Physiological properties, time of development, and central
753   projection are correlated in the wing mechanoreceptors of Drosophila. *J Neurosci* 7:4201–
754   4208. doi:10.1523/jneurosci.07-12-04201.1987

755   Eichel MA, Gargareta V-I, D'Este E, Fledrich R, Kungl T, Buscham TJ, Lüders KA, Miracle C,
756   Jung RB, Distler U, Kusch K, Möbius W, Hülsmann S, Tenzer S, Nave K-A, Werner HB.
757   2020. CMTM6 expressed on the adaxonal Schwann cell surface restricts axonal diameters in
758   peripheral nerves. *Nat Commun* 11:4514. doi:10.1038/s41467-020-18172-7

759   Feltri ML, Porta DG, Previtali SC, Nodari A, Migliavacca B, Cassetti A, Littlewood-Evans A,
760   Reichardt LF, Messing A, Quattrini A, Mueller U, Wrabetz L. 2002. Conditional disruption of
761   beta 1 integrin in Schwann cells impedes interactions with axons. *The Journal of cell biology*
762   156:199–209. doi:10.1083/jcb.200109021

763 Franco-Pons N, Tomàs J, Roig B, Auladell C, Martorell L, Vilella E. 2009. Discoidin domain
764   receptor 1, a tyrosine kinase receptor, is upregulated in an experimental model of
765   remyelination and during oligodendrocyte differentiation in vitro. *Journal of molecular*
766   *neuroscience : MN* 38:2–11. doi:10.1007/s12031-008-9151-x

767 Franco-Pons N, Virgos C, Vogel WF, Ureña JM, Soriano E, Rio JA del, Vilella E. 2006.
768   Expression of discoidin domain receptor 1 during mouse brain development follows the
769   progress of myelination. *Neuroscience* 140:463–475. doi:10.1016/j.neuroscience.2006.02.033

770 Franzdóttir SR, Engelen D, Yuva-Aydemir Y, Schmidt I, Aho A, Klämbt C. 2009. Switch in
771   FGF signalling initiates glial differentiation in the Drosophila eye. *Nature* 460:758–761.
772   doi:10.1038/nature08167

773 Furusho M, Dupree JL, Bryant M, Bansal R. 2009. Disruption of fibroblast growth factor
774   receptor signaling in nonmyelinating Schwann cells causes sensory axonal neuropathy and
775   impairment of thermal pain sensitivity. *The Journal of neuroscience : the official journal of*
776   *the Society for Neuroscience* 29:1608–1614. doi:10.1523/jneurosci.5615-08.2009

777 Garbern JY, Yool DA, Moore GJ, Wilds IB, Faulk MW, Klugmann M, Nave K, Sistermans EA,
778   Knaap MS van der, Bird TD, Shy ME, Kamholz JA, Griffiths IR. 2002. Patients lacking the
779   major CNS myelin protein, proteolipid protein 1, develop length-dependent axonal
780   degeneration in the absence of demyelination and inflammation. *Brain* 125:551–561.
781   doi:10.1093/brain/awf043

782 Gas C, Canales-Rodríguez EJ, Radua J, Abasolo N, Cortés MJ, Salvadó E, Muntané G, Alemán-
783   Gómez Y, Julià T, Marsal S, Sanjuan J, Guitart M, Costas J, Martorell L, Pomarol-Clotet E,
784   Vilella E. 2018. Discoidin domain receptor 1 gene variants are associated with decreased
785   white matter fractional anisotropy and decreased processing speed in schizophrenia. *J*
786   *Psychiatr Res* 110:74–82. doi:10.1016/j.jpsychires.2018.12.021

787 Gerber D, Pereira JA, Gerber J, Tan G, Dimitrieva S, Yángüez E, Suter U. 2021. Transcriptional
788   profiling of mouse peripheral nerves to the single-cell level to build a sciatic nerve ATlas
789   (SNAT). *Elife* 10:e58591. doi:10.7554/elife.58591

790 Ghosh A, Kling T, Snaidero N, Sampaio JL, Shevchenko A, Gras H, Geurten B, Göpfert MC,
791   Schulz JB, Voigt A, Simons M, Perrimon N. 2013. A Global In Vivo Drosophila RNAi
792   Screen Identifies a Key Role of Ceramide Phosphoethanolamine for Glial Ensheathment of
793   Axons. *PLoS genetics* 9:e1003980. doi:10.1371/journal.pgen.1003980.s012

794 Gohl DM, Silies MA, Gao XJ, Bhalerao S, Luongo FJ, Lin C-C, Potter CJ, Clandinin TR. 2011.
795   A versatile in vivo system for directed dissection of gene expression patterns. *Nature methods*
796   8:231–237.

797 Griffin JW, Thompson WJ. 2008. Biology and pathology of nonmyelinating Schwann cells. *Glia*
798   56:1518–1531. doi:10.1002/glia.20778

799 Griffiths I, Klugmann M, Anderson T, Yool D, Thomson C, Schwab MH, Schneider A,
800   Zimmermann F, McCulloch M, Nadon N, Nave KA. 1998. Axonal swellings and
801   degeneration in mice lacking the major proteolipid of myelin. *Science (New York, NY)*
802   280:1610–1613.

803 Hilchen CM von, Bustos AE, Giangrande A, Technau GM, Altenhein B. 2013. Predetermined
804   embryonic glial cells form the distinct glial sheaths of the Drosophila peripheral nervous
805   system. *Development (Cambridge, England)*. doi:10.1242/dev.093245

806 Hsieh S, Kidd G, Crawford T, Xu Z, Lin W, Trapp B, Cleveland D, Griffin J. 1994. Regional
807   modulation of neurofilament organization by myelination in normal axons. *J Neurosci*
808   14:6392–6401. doi:10.1523/jneurosci.14-11-06392.1994

809 Hsu J-M, Kang Y, Corty MM, Mathieson D, Peters OM, Freeman MR. 2021. Injury-Induced
810   Inhibition of Bystander Neurons Requires dSarm and Signaling from Glia. *Neuron* 109:473-
811   487.e5. doi:10.1016/j.neuron.2020.11.012

812 Klugmann M, Schwab MH, Pühlhofer A, Schneider A, Zimmermann F, Griffiths IR, Nave K-A.
813   1997. Assembly of CNS Myelin in the Absence of Proteolipid Protein. *Neuron* 18:59–70.
814   doi:10.1016/s0896-6273(01)80046-5

815 Kottmeier R, Bittern J, Schoofs A, Scheiwe F, Matzat T, Pankratz M, Klämbt C. 2020. Wrapping
816   glia regulates neuronal signaling speed and precision in the peripheral nervous system of
817   Drosophila. *Nat Commun* 11:4491. doi:10.1038/s41467-020-18291-1

818 Lappe-Siefke C, Goebbels S, Gravel M, Nicksch E, Lee J, Braun PE, Griffiths IR, Nave K-A.
819   2003. Disruption of Cnp1 uncouples oligodendroglial functions in axonal support and
820   myelination. *Nature genetics* 33:366–374. doi:10.1038/ng1095

821 Larkin A, Marygold SJ, Antonazzo G, Attrill H, dos Santos G, Garapati PV, Goodman JL,
822   Gramates LS, Millburn G, Strelets VB, Tabone CJ, Thurmond J, Consortium F, Perrimon N,
823   Gelbart SR, Agapite J, Broll K, Crosby M, Santos G dos, Falls K, Gramates LS, Jenkins V,
824   Longden I, Matthews B, Sutherland C, Tabone CJ, Zhou P, Zytkovicz M, Brown N,
825   Antonazzo G, Attrill H, Garapati P, Larkin A, Marygold S, McLachlan A, Millburn G,
826   Pilgrim C, Ozturk-Colak A, Trovisco V, Kaufman T, Calvi B, Goodman J, Strelets V,
827   Thurmond J, Cripps R, Lovato T. 2020. FlyBase: updates to the Drosophila melanogaster
828   knowledge base. *Nucleic Acids Res* 49:D899–D907. doi:10.1093/nar/gkaa1026

829 Luan H, Peabody NC, Vinson CR, White BH. 2006. Refined spatial manipulation of neuronal
830   function by combinatorial restriction of transgene expression. *Neuron* 52:425–436.
831   doi:10.1016/j.neuron.2006.08.028

832 Lyons DA, Pogoda H-M, Voas MG, Woods IG, Diamond B, Nix R, Arana N, Jacobs J, Talbot
833   WS. 2005. erbb3 and erbb2 are essential for schwann cell migration and myelination in
834   zebrafish. *Current biology : CB* 15:513–524. doi:10.1016/j.cub.2005.02.030

835   Matzat T, Sieglitz F, Kottmeier R, Babatz F, Engelen D, Klämbt C. 2015. Axonal wrapping in
836   the Drosophila PNS is controlled by glia-derived neuregulin homolog Vein. *Development*
837   *(Cambridge, England)* 142:1336–1345. doi:10.1242/dev.116616

838   Meyer F, Moussian B. 2009. Drosophila multiplexin (Dmp) modulates motor axon pathfinding
839   accuracy. *Development, growth & differentiation* 51:483–498. doi:10.1111/j.1440-
840   169x.2009.01111.x

841   Michailov GV, Sereda MW, Brinkmann BG, Fischer TM, Haug B, Birchmeier C, Role L, Lai C,
842   Schwab MH, Nave K-A. 2004. Axonal Neuregulin-1 Regulates Myelin Sheath Thickness.
843   *Science* 304:700–703. doi:10.1126/science.1095862

844   Monk KR, Feltri ML, Taveggia C. 2015. New insights on schwann cell development. *Glia*.
845   doi:10.1002/glia.22852

846   Mukherjee C, Kling T, Russo B, Miebach K, Kess E, Schifferer M, Pedro LD, Weikert U, Fard
847   MK, Kannaiyan N, Rossner M, Aicher M-L, Goebbels S, Nave K-A, Krämer-Albers E-M,
848   Schneider A, Simons M. 2020. Oligodendrocytes Provide Antioxidant Defense Function for
849   Neurons by Secreting Ferritin Heavy Chain. *Cell Metab* 32:259-272.e10.
850   doi:10.1016/j.cmet.2020.05.019

851   Myllyharju J, Kivirikko KI. 2004. Collagens, modifying enzymes and their mutations in humans,
852   flies and worms. *Trends Genet* 20:33–43. doi:10.1016/j.tig.2003.11.004

853   Nave K-A. 2010. Myelination and support of axonal integrity by glia. *Nature* 468:244–252.
854   doi:10.1038/nature09614

855   Neukomm LJ, Burdett TC, Gonzalez MA, Züchner S, Freeman MR. 2014. Rapid in vivo forward
856   genetic approach for identifying axon death genes in Drosophila. *Proceedings of the National*
857   *Academy of Sciences* 111:9965–9970. doi:10.1073/pnas.1406230111

858   Ochoa J, Mair WG. 1969. The normal sural nerve in man. I. Ultrastructure and numbers of fibres
859   and cells. *Acta neuropathologica* 13:197–216.

860   Orita S, Henry K, Mantuano E, Yamauchi K, Corato AD, Ishikawa T, Feltri ML, Wrabetz L,
861   Gaultier A, Pollack M, Ellisman M, Takahashi K, Gonias SL, Campana WM. 2013. Schwann
862   cell LRP1 regulates remak bundle ultrastructure and axonal interactions to prevent
863   neuropathic pain. *The Journal of neuroscience : the official journal of the Society for*
864   *Neuroscience* 33:5590–5602. doi:10.1523/jneurosci.3342-12.2013

865   Pereira JA, Benninger Y, Baumann R, Gonçalves AF, Ozçelik M, Thurnherr T, Tricaud N,
866   Meijer D, Fässler R, Suter U, Relvas JB. 2009. Integrin-linked kinase is required for radial
867   sorting of axons and Schwann cell remyelination in the peripheral nervous system. *The*
868   *Journal of cell biology* 185:147–161. doi:10.1083/jcb.200809008

869 Petersen SC, Luo R, Liebscher I, Giera S, Jeong S-J, Mogha A, Ghidinelli M, Feltri ML,
870   Schöneberg T, Piao X, Monk KR. 2015. The adhesion GPCR GPR126 has distinct, domain-
871   dependent functions in Schwann cell development mediated by interaction with laminin-211.
872   *Neuron* 85:755–769. doi:10.1016/j.neuron.2014.12.057

873 Petley-Ragan LM, Ardiel EL, Rankin CH, Auld VJ. 2016. Accumulation of Laminin Monomers
874   in Drosophila Glia Leads to Glial Endoplasmic Reticulum Stress and Disrupted Larval
875   Locomotion. *Journal of Neuroscience* 36:1151–1164. doi:10.1523/jneurosci.1797-15.2016

876 Potter CJ, Tasic B, Russler EV, Liang L, Luo L. 2010. The Q system: a repressible binary system
877   for transgene expression, lineage tracing, and mosaic analysis. *Cell* 141:536–548.
878   doi:10.1016/j.cell.2010.02.025

879 Rasi K, Hurskainen M, Kallio M, Stavén S, Sormunen R, Heape AM, Avila RL, Kirschner D,
880   Muona A, Tolonen U, Tanila H, Huhtala P, Soininen R, Pihlajaniemi T. 2010. Lack of
881   collagen XV impairs peripheral nerve maturation and, when combined with laminin-411
882   deficiency, leads to basement membrane abnormalities and sensorimotor dysfunction. *The
883   Journal of neuroscience : the official journal of the Society for Neuroscience* 30:14490–
884   14501. doi:10.1523/jneurosci.2644-10.2010

885 Risse B, Berh D, Otto N, Klämbt C, Jiang X. 2017. FIMTrack: An open source tracking and
886   locomotion analysis software for small animals. *PLoS computational biology* 13:e1005530.
887   doi:10.1371/journal.pcbi.1005530

888 Roig B, Franco-Pons N, Martorell L, Tomàs J, Vogel WF, Vilella E. 2010. Expression of the
889   tyrosine kinase discoidin domain receptor 1 (DDR1) in human central nervous system myelin.
890   *Brain research* 1336:22–29. doi:10.1016/j.brainres.2010.03.099

891 Saab AS, Tzvetavona ID, Trevisiol A, Baltan S, Dibaj P, Kusch K, Möbius W, Goetze B, Jahn
892   HM, Huang W, Steffens H, Schomburg ED, Pérez-Samartín A, Pérez-Cerdá F, Bakhtiari D,
893   Matute C, Löwel S, Griesinger C, Hirrlinger J, Kirchhoff F, Nave K-A. 2016.
894   Oligodendroglial NMDA Receptors Regulate Glucose Import and Axonal Energy
895   Metabolism. *Neuron* 91:119–132. doi:10.1016/j.neuron.2016.05.016

896 Schmalbruch H. 1986. Fiber composition of the rat sciatic nerve. *The Anatomical record* 215:71–
897   81. doi:10.1002/ar.1092150111

898 Snaidero N, Velte C, Myllykoski M, Raasakka A, Ignatev A, Werner HB, Erwig MS, Möbius W,
899   Kursula P, Nave K-A, Simons M. 2017. Antagonistic Functions of MBP and CNP Establish
900   Cytosolic Channels in CNS Myelin. *Cell Reports* 18:314–323.
901   doi:10.1016/j.celrep.2016.12.053

902 Stassart RM, Fledrich R, Velanac V, Brinkmann BG, Schwab MH, Meijer D, Sereda MW, Nave
903   K-A. 2013. A role for Schwann cell-derived neuregulin-1 in remyelination. *Nature
904   neuroscience* 16:48–54. doi:10.1038/nn.3281

905 Stassart RM, Möbius W, Nave K-A, Edgar JM. 2018. The Axon-Myelin Unit in Development
906 and Degenerative Disease. *Front Neurosci-switz* 12:467. doi:10.3389/fnins.2018.00467

907 Stork T, Engelen D, Krudewig A, Silies M, Bainton RJ, Klämbt C. 2008. Organization and
908 function of the blood-brain barrier in Drosophila. *The Journal of neuroscience : the official*
909 *journal of the Society for Neuroscience* 28:587–597. doi:10.1523/jneurosci.4367-07.2008

910 Taveggia C, Zanazzi G, Petrylak A, Yano H, Rosenbluth J, Einheber S, Xu X, Esper RM, Loeb
911 JA, Shrager P, Chao MV, Falls DL, Role L, Salzer JL. 2005. Neuregulin-1 type III determines
912 the ensheathment fate of axons. *Neuron* 47:681–694. doi:10.1016/j.neuron.2005.08.017

913 Viader A, Golden JP, Baloh RH, Schmidt RE, Hunter DA, Milbrandt J. 2011. Schwann Cell
914 Mitochondrial Metabolism Supports Long-Term Axonal Survival and Peripheral Nerve
915 Function. *J Neurosci* 31:10128–10140. doi:10.1523/jneurosci.0884-11.2011

916 Viader A, Sasaki Y, Kim S, Strickland A, Workman CS, Yang K, Gross RW, Milbrandt J. 2013.
917 Aberrant Schwann cell lipid metabolism linked to mitochondrial deficits leads to axon
918 degeneration and neuropathy. *Neuron* 77:886–898. doi:10.1016/j.neuron.2013.01.012

919 Vogel W, Gish GD, Alves F, Pawson T. 1997. The discoidin domain receptor tyrosine kinases
920 are activated by collagen. *Molecular cell* 1:13–23.

921 Waegh SM de, Lee VM-Y, Brady ST. 1992. Local modulation of neurofilament
922 phosphorylation, axonal caliber, and slow axonal transport by myelinating Schwann cells.
923 *Cell* 68:451–463. doi:10.1016/0092-8674(92)90183-d

924 Wang T, Hauswirth AG, Tong A, Dickman DK, Davis GW. 2014. Endostatin Is a Trans-
925 Synaptic Signal for Homeostatic Synaptic Plasticity. *Neuron* 83:616–629.
926 doi:10.1016/j.neuron.2014.07.003

927 Wang T, Morency DT, Harris N, Davis GW. 2019. Epigenetic Signaling in Glia Controls
928 Presynaptic Homeostatic Plasticity. *Neuron* 105:491-505.e3.
929 doi:10.1016/j.neuron.2019.10.041

930 Xie X, Auld VJ. 2011. Integrins are necessary for the development and maintenance of the glial
931 layers in the Drosophila peripheral nerve. *Development (Cambridge, England)* 138:3813–
932 3822. doi:10.1242/dev.064816

933 Yin X, Crawford TO, Griffin JW, Tu P h, Lee VM, Li C, Roder J, Trapp BD. 1998. Myelin-
934 associated glycoprotein is a myelin signal that modulates the caliber of myelinated axons. *J*
935 *Neurosci* 18:1953–1962. doi:10.1523/jneurosci.18-06-01953.1998

936 Yu W-M, Yu H, Chen Z-L, Strickland S. 2009. Disruption of laminin in the peripheral nervous
937 system impedes nonmyelinating Schwann cell development and impairs nociceptive sensory
938 function. *Glia* 57:850–859. doi:10.1002/glia.20811

939   Zhang Y, Chen K, Sloan SA, Bennett ML, Scholze AR, O'Keeffe S, Phatnani HP, Guarnieri P,
940   Caneda C, Ruderisch N, Deng S, Liddelow SA, Zhang C, Daneman R, Maniatis T, Barres
941   BA, Wu JQ. 2014. An RNA-Sequencing Transcriptome and Splicing Database of Glia,
942   Neurons, and Vascular Cells of the Cerebral Cortex. *The Journal of neuroscience : the official*
943   *journal of the Society for Neuroscience* 34:11929–11947. doi:10.1523/jneurosci.1860-
944   14.2014

945   Zöller I, Meixner M, Hartmann D, Büssow H, Meyer R, Gieselmann V, Eckhardt M. 2008.
946   Absence of 2-Hydroxylated Sphingolipids Is Compatible with Normal Neural Development
947   But Causes Late-Onset Axon and Myelin Sheath Degeneration. *J Neurosci* 28:9741–9754.
948   doi:10.1523/jneurosci.0458-08.2008

949